

**The Space-Time Picture of the Wee Partons
and
the AGK Cutting Rules in Perturbative QCD**

J.Bartels¹

II Institut für Theoretische Physik, Universität Hamburg,
D-22761 Hamburg, Germany.

M.G.Ryskin²

St.Petersburg Nuclear Physics Institute
188350, Gatchina, S.Petersburg, Russia

Abstract: We discuss the space-time picture of scattering amplitudes with single and double ladder exchange in perturbative QCD. Particular emphasis is given to the Abramovsky Gribov Kanchelli (AGK) rules which describe the relative contributions of the diffractive dissociation and processes with other multiplicities to the elastic scattering amplitude. Inside the Pomeron Pomeron interaction vertices we find a new matrix which describes the transition from one s-cut to another and which goes beyond the original the AGK rules.

¹Supported by Bundesministerium für Forschung und Technologie, Bonn, Germany under Contract 05 6HH93P(5) and EEC Program "Human Capital and Mobility" through Network "Physics at High Energy Colliders" under Contract CHRX-CT93-0357 (DG12 COMA).

²This is work supported in part by the Grant INTAS-93-0079 and by the Volkswagen Stiftung.

1 Introduction

The role of the space-time structure of reggeon exchanges in developing a physical picture of high energy hadron scattering has been recognized many years ago[1]. The most important result was given in a paper by Abramovski, Gribov, Kancheli (AGK) [2], where the so-called “cutting rules“ both for unenhanced reggeon diagrams and for the triple pomeron vertex were derived. These rules state the ratios between the different types of reggeon cuts, i.e. between the processes with different multiplicities (secondary particle densities) in the high energy interactions. In the present paper we will discuss how these “old ideas“ are realized in perturbative QCD.

Recent interest in this question comes from deep inelastic scattering at small x and, in particular, from the observation of events with a large rapidity gap between the diffractively excited state of the virtual photon and the outgoing proton. It is commonly felt that the latter process is most easily described in the proton rest frame, and it seems useful to develop an intuitive picture of the space-time evolution of this very interesting reaction. Even if the Pomeron in this process is, at best, only partly perturbative and has a strong nonperturbative component, we nevertheless expect that the basic space time structure may be correctly predicted by the perturbative analysis. In any case, the observation of diffraction dissociation of the photon at HERA indicates that unitarity corrections (double ladder exchange) to the standard one-ladder description of F_2 are present: the AGK rules tell us how such a diffractive state contributes to the double ladder exchange in the elastic process $\gamma^* + p \rightarrow \gamma^* + p$, i.e. they provide a connection between this particular final state and the first unitarity corrections to F_2 . On the other hand, from these rules it is not immediately obvious how to combine the space-time picture of the diffractive dissociation process with that of the elastic process $\gamma^* + p \rightarrow \gamma^* + p$. A careful analysis of perturbative QCD allows to answer these questions.

Throughout this paper it will be crucial to distinguish between scattering amplitudes and their imaginary parts (energy discontinuities). In particular, the space-time structure of a scattering amplitude and the question for intermediate states are, although closely connected, not exactly the same. Namely, a space-time analysis of a perturbative *scattering amplitude* proceeds as follows: rather than using the usual (covariant) Feynman rules for evaluating diagrams, one decomposes the Feynman amplitudes into pieces with different time orderings (“old fashioned perturbation theory“). At high energies it can then be shown that the leading contribution arises only from a specific subset of the different time orderings, and in this way a natural space time picture of the scattering process emerges. If, on the other hand, one wants to know which *intermediate physical states* correspond to this scattering process, one has to analyse, because of unitarity, the *imaginary part* (more general: the energy discontinuity) of the scattering amplitude. For individual Feynman diagrams, one very often finds cancellations between different contributions to the energy discontinuity; a famous example is the AFS cancellation [3, 4] in planar two ladder exchange diagrams which we will have to briefly recapitulate. As a result of these cancellations, the scattering amplitude may look somewhat simpler and may lead to the (false) impression that certain intermediate states do not exist. For reggeon diagrams, the AGK rules state in a simple way which intermediate states exist and what relative weight they have in an elastic scattering amplitude. It is possible to give a space-time picture also for these imaginary parts of a scattering amplitude, but it is somewhat less intuitive. In this paper we will illustrate all these aspects for QCD reggeon diagrams with two or four reggeized gluons in the t-channel. As a specific example, we have in mind the process $\gamma^* + p \rightarrow \gamma^* + p$ and the diffractive dissociation of the photon.

The outline of this paper is the following. In sect.2 we briefly review the space-time picture of a simple ladder exchange in the elastic two-body scattering amplitude, as it has been derived many years ago in the leading logarithmic approximation of the scalar $\lambda\phi^3$ field theory. Although, at first sight, the situation in QCD may seem to be infinitely more complicated, the leading logarithmic approximation, the BFKL Pomeron [5], is in complete agreement with this old and simple picture. This is mainly due to the fact that all Feynman diagrams that contribute to this approximation can be cast into the ladder structure with *effective* vertices and kernels (rungs), and for these elements the region of integration is analogous to the scalar ladders. For our present purposes we therefore feel that we may skip details of the BFKL calculations and simply describe the results in terms of the simple scalar ladder structure. The main new aspect, which is introduced by QCD and has not been discussed before, is the reggeization of the gluon. Due to the color degrees of freedom we have to consider both positive and negative signature of the exchange channel. All this discussion of the elastic $2 \rightarrow 2$ scattering process can easily be generalized to the process of the diffractive dissociation.

In the following section 3 we discuss the space-time structure of the double ladder exchange scattering amplitude and, more general, reggeon diagrams with up to four reggeons in the t-channel, very much in the same spirit as the single ladder. When iterating the two-ladder exchange in the t-channel we find the new phenomenon of the “change of the arrows“ of the flow of momenta across the diagrams. With this new element we are able to give a complete space-time picture of QCD diagrams with two and four gluons in the t-channel.

In sections 4 and 5 we turn to the analysis of intermediate states of these QCD diagrams. We begin with a brief review of the AGK rules, applied to the two ladder exchange. In sections 5 we illustrate the AGK rules for the QCD case. We perform an analysis of the imaginary parts of diagrams with two and four gluons in the t-channel, and we explain how the AGK rules are satisfied. Particular attention is, again, given to the interaction between two ladders: we obtain ratios of the different cuts across the interaction vertex. These relations are new and have never been discussed in “old“ reggeon theory.

2 Space-time structure of the leading diagrams

2.1 Elastic Scattering of a Virtual Photon

In the leading log approximation the high energy behavior is dominated by ladder diagrams (throughout this paper the term “leading log“ will always refer to the total energy of the process under consideration). The simplest example (for a scalar theory) is shown in Fig.1a. What we have in mind is the elastic scattering of a virtual photon with momentum q^μ off a hadron target (momentum p^μ). Strictly speaking, the cleanest laboratory for investigating the high energy limit of perturbative QCD would be the elastic scattering of two virtual photons. On the other hand, we expect that the space-time structure as well as the AGK-rules will not be altered if we replace the target virtual photon by a proton: throughout this paper we will assume that this lower part of our scattering amplitude, although perturbative QCD is not applicable, will have the same general features as obtained from perturbative QCD. The coupling of the gluon ladder to the virtual photon is through a quark loop. Since at high energies this quark loop never produces any logarithm of the

energy, it appears as an energy independent “form factor“ with some dependence on the transverse momenta of the gluon legs. For most of our discussion it will be sufficient to replace the quark loop by a parton line. Throughout this paper energy $s = Q^2/x_B$ will be assumed to be large, i.e. x_B very small. In order to illustrate the space time structure we will make a further step of simplification: instead of QCD diagrams with quarks and gluons we will begin with (massive) scalar diagrams.

We will use Sudakov (light-cone) variables

$$q_{i,\mu} = \alpha_i q'_\mu + \beta_i p'_\mu + q_{i,t,\mu}; \quad d^4 q_i = \frac{1}{2} s d\alpha_i d\beta_i d^2 q_{i,t}; \quad s = 2p'q'$$

$$q^2 = -Q^2; \quad q' = q + x_B p', \quad p' \approx p; \quad q'^2 = p'^2 = 0 \quad (1)$$

(note that, in this notation, $q_t^2 < 0$; transverse momentum is defined as $\mathbf{q}^2 = -q_t^2$). The typical structure of the leading logarithmic longitudinal integration leads to the following ordering of the α_i in the interval from 0 to 1:

$$0 \ll \alpha_n \ll \dots \ll \alpha_2 \ll \alpha_1 \ll 1. \quad (2)$$

Due to the momentum conservation we have approximately $\alpha_{(q)i} \approx \alpha_{(k)i} = \alpha_i$. Then in each β_i cell one can close the contour of the integration in the lower half plane, where the only pole comes from the propagator of the rung $1/(q_i^2 - m^2 + i\epsilon) = 1/(s\alpha_i\beta_i + q_{it}^2 - m^2 + i\epsilon)$ ³, and one obtains $\beta_i = (m^2 - q_{it}^2 - i\epsilon)/s\alpha_i$. As a result of the α_i -ordering (2), also the β_i are ordered, but in the opposite direction:

$$0 \ll \beta_1 \ll \dots \ll \beta_{n-1} \ll \beta_n \ll 1. \quad (3)$$

From (3) it follows that $\beta_{(q)i} \approx \beta_{(k)i+1} = \beta_i$. The last s-channel pole (the rung at the bottom of Fig.1a) $1/(q_n^2 - m^2)$ is used for the α_n integration (because of the symmetry between the α_i and the β_i , we also could have started with (3), then performed the α_i integrals and ended with the ordering prescription (2). We then would be left with the β_1 -integral and the rung at the top of Fig.1a). For an amplitude with the positive signature (say, pomeron exchange) we have to sum up the graphs Fig.1a and 1b. In this sum the leading logs in the real part - $\int d\alpha_n (\frac{1}{\alpha_n s + i\epsilon} + \frac{1}{-\alpha_n s + i\epsilon})$ - cancels, and the main contribution comes from the imaginary part of the propagator $\frac{1}{\alpha_n s + q_{in}^2 - m^2 + i\epsilon} = -i\pi\delta(\alpha_n s + q_{nt}^2 - m^2)$. Thus all the s-channel particles are on mass shell. We finally note that if one chooses $\alpha_1 > 1$, or violates the ordering eq.(2), all poles of one (or more) of the β_i variables would be on the same side of the integration contour, and the integral would vanish.

Let us now consider the same ladder diagrams in “old-fashioned“ (noncovariant) perturbation theory in the target rest frame ($p_\mu = (m_N, 0, 0, 0)$, $q'_\mu = (Q^2/2x_B m_N, 0, 0, Q^2/2x_B m_N)$). “Time“ runs from the left to right, and we draw the vertices in a time-ordered way. In the high energy limit only the time ordering shown in Fig.2a survives. For each intermediate state we draw a cutting line (Fig.2a), and we have to integrate over the time difference $\tau = t_i - t_{i-1}$:

$$\frac{1}{2E_i} \int_0^\infty e^{i(E_{cut,i} - q_0 + i\epsilon)\tau} d\tau \quad (4)$$

³For the β_i -loop, this pole is the only one in the lower half plane; this is because of the positive sign of α_i . The other three propagators of this loop have the opposite time direction (i.e. the opposite α direction), and their poles are in the upper half plane.

Here $E_{cut,i}$ stands for the sum of the energies of all lines that belong to the intermediate state, q_0 for the energy of the incoming photon, and the life-time corresponding to the cut state is proportional to $1/(E_{cut,i} - q_0)$. In the high energy approximation the energy of a parton with momentum k_i is given by $E_i \sim k_{iz} + \frac{\mathbf{k}_i^2 + m^2}{2E_i}$. Due to the momentum conservation in $E_{cut,i} - q_0$ the 3-components drop out, and in the remainder the line with the smallest energy dominates. Making use of $E_i \approx \alpha_i q'_0$ and the ordering condition (2) one sees that the life time of the intermediate state in Fig.2a is proportional to the energy of the parton with momentum k_i , i.e. $\tau_i \sim \alpha_i Q^2 / 2x_B (\mathbf{k}_i^2 + m^2) m_N$. For the the central cut which “runs through the target“ we have the energy difference $\sum E_i - E_{q+p}$: from the analysis above we know that all produced particles are on-mass shell, and $\sum E_i = E_{p+q}$. Hence there is no limit on the life time of the central cut, i.e. this state can live for a long time. For the parton life times before the interaction we have the ordering condition:

$$\tau_n \ll \tau_{n-1} \ll \dots \ll \tau_1 \quad (5)$$

(similarly for the life times after the interactions), i.e. the parton closest to the incident photon has the longest life-time.

It is instructive to interpret the same Feynman diagrams also in another reference frame, e.g. the Breit frame (“photon rest frame“) where the four momentum of the proton has the form $q^\mu = (0, 0, 0, \sqrt{Q^2})$. This is the frame where the partonic interpretation of deep inelastic scattering is most easily obtained. It is now the partons close to the fast proton which have the longest life-time, since in this case the energy of the i -th parton is mainly given by the β_i -component of the momentum q_i , which according to (2) increase with i . Therefore in this frame $\tau_i \approx 2E_i / (\mathbf{k}_i^2 + m^2) \propto \beta_i$, and the parton with the longest lifetime is the one at the bottom of the diagram. Consequently, in this frame the proton splits into partons which have smaller and smaller longitudinal momenta β_i , and the photon finally interacts with the parton for which $\beta = x_B$.

Needless to say that the physics of the process does not change if we perform a simple Lorentz boost: in each frame we encounter the feature that the fastest parton has the longest lifetime. In the proton rest system we probe the partons with small momentum fraction α inside the photon, in the Breit system those with small β inside the proton. If we choose a frame in between, e.g. the CM system, it is the interaction of the small- α partons from the photon with the small- β partons from the proton (see Fig.2b).

It should be stressed that, up to now, the discussion of the space-time structure holds for the scattering amplitude and not for the imaginary part. This follows from the observation that the direction of time is determined by the relative sign of α and $i\epsilon$. For the elastic amplitude (Fig.1a) the space time picture looks as Fig.2a. In order to get a precise information on what kind of intermediate state is contained in our amplitude, we have to ask for cross sections which, via the unitarity equations, are related to the energy discontinuity. The space-time picture then becomes quite different: if, for example, we cut the ladders as indicated in Fig.3a, the time to the right of the cutting line goes in the backward (inverse) direction. This part of the diagram now corresponds to the complex conjugate amplitude A^* and, hence, it has the opposite sign of the $i\epsilon$'s in the $1/k_i'^2$ propagators. In other words, the cut diagram Fig.3a reflects the space-time structure of the $2 \rightarrow n + 1$ matrix element squared. To say this in different words: taking the discontinuity of the scattering amplitude is like “interrupting the time evolution at a certain time“ and then reversing the direction of time (Fig.3b) . This point was discussed in more detail in the appendix of ref.[6].

Since QCD contains, in addition to the even signature Pomeron exchange, also the reggeizing gluon with odd signature, a few words have to be said about the graphs which describe the exchange of a reggeized gluon. Because of the famous bootstrap property (for further discussion see section 5), the exchange of a single reggeized gluon is identical to ladder diagrams in the color octet representation. The simplest diagram of such a type is, again, a ladder of the type Fig.1a,b. But now, in contrast to the even signature (Pomeron) case, where we take the sum of the ladder and its crossed counterpart (Fig.1a and Fig.1b) now we deal with the difference ($\frac{1}{\alpha_n s} - \frac{1}{-\alpha_n s}$). This simple difference leads to a change in the space-time structure. Namely now the α_n integral from the lowest rung gives a logarithm which is not cancelled by the crossed diagram, and it comes from a region of integration where the virtuality of this rung is large, i.e. in contrast to the even signature case there is now one rung off its mass shell. In order to obtain the correct interpretation of this effect we have again to study the space-time picture (Fig.2a). The major change compared to the even signature state is results from the off-shellness of the lowest rung: now we have no longer the equality $\sum E_i = E_{p+q}$, and the time integral belonging to the central cut leads to finite lifetime $\Delta\tau \sim 1/(\sum E_i - E_{p+q}) \approx \alpha_n s$. So the life time of the full odd signature ladder is substantially smaller than that of an even signature ladder. This difference becomes particularly acute if we consider a reggeized gluon inside a larger diagram (Fig.4). Although inside this ladder we have the usual ordering of life-times, compared to its “environment“ the ladder represents only a short-lived fluctuation. Therefore, as far as the leading real part of this subamplitude is concerned one can consider this ladder as a single object – as a reggeized gluon. However, if we consider the (non-leading) imaginary part of the reggeon, which corresponds to the discontinuity of the propagator $i\pi\delta(m^2 - q_n^2)$ at the bottom of the ladder one loses one energy logarithm and has again the normal time-life $\tau_i \sim E_i/(m^2 + \mathbf{k}_i^2)$.

So far we have used scalar field theory to illustrate the space time structure of Feynman diagrams in the high energy limit. As we said in the introduction, this structure holds also for the QCD scattering amplitude if we simply replace the line of the incoming particle by a quark-antiquark pair, the ladder rungs by BFKL kernels, and t-channel scalar particles by reggeized gluons.

2.2 Diffractive Dissociation

Now let us consider the scattering amplitude of the diffractive dissociation of the beam particle. To be definite, we consider the dissociation of the virtual photon into a system with fixed mass M ($M^2 \ll s$ which consists of a $q\bar{q}$ pair plus a few gluons (Fig.5a). As before, we begin with the rest frame of the target proton. The corresponding picture is shown in Fig.5b. The largest time is the formation time of the particles in the diffracted system M^2 ; the quarks have the largest values of $\alpha_i \sim O(1)$. The gluon emitted from the quark has already a smaller α , but it is still larger than that of gluon with momentum k etc. The time interval occupied by the t-channel pomeron is controlled by the life-time of the gluon with momentum k ; its energy is the same as that of the rung with q . Hence $\tau_k \propto \alpha q_0/\mathbf{q}^2$. It is even better to express the time τ in terms of the β_i variables, which denote the momentum fraction of the proton momentum p_μ carried away by the parton-i. As $\beta_i = \mathbf{q}_i^2/\alpha_i s$, we have [7] $\tau_i \sim 1/\beta_i m_N = 1/x_i m_N$, where m_N is the nucleon (target) mass. It should be stressed that while at the bottom of the graph (Fig.5b) the time and the z longitudinal intervals are small (of the order of proton radius; as the corresponding x_i here are large enough

($\sim 0.3 - 0.1$) and $\tau \simeq 1/x_i m_N \sim 1Fm$), the gluon at the top of the ladder needs a rather long time $\sim 1/x_P m_N$ ($x_P \ll 1$) to recollect all the partons which have been emitted inside the Pomeron ladder.

The picture looks quite different in the Breit frame where the proton is fast and the beam “is at rest“ (Fig.5c). The first impression is that now the partons produced inside the Pomeron belong to the fast proton. Nevertheless, it is exactly the same Feynman graph as in Fig.5a. Our different ways of re-drawing the same Feynman diagrams only illustrate that any interpretation involving “time“ is not Lorentz invariant and hence changes from the one reference frame to another. In the Breit frame $\tau \propto \beta_i$, and the time interval at the bottom of the pomeron ladder is the largest one, but even at the upper end of the pomeron the life-time of the highest parton with momentum fraction x_1 is larger than the formation time for the particles in the diffracted system M^2 . However these particles will be detected far away from the interaction point and they do have time enough to absorb (interact with the) our ‘non-local’ pomeron.

3 Diagrams with Two or Four t-Channel Gluons

Having demonstrated that amplitudes for both the elastic process $\gamma^* + p \rightarrow \gamma^* + p$ and the diffractive process $\gamma^* + p \rightarrow M + p$ have a simple space time interpretation, it seems most natural to ask how the latter process contributes to the total cross section $\gamma^* + p$ which is given by the imaginary part (or the energy discontinuity) of the elastic scattering amplitude for $\gamma^* + p$. This leads us to a study of higher order corrections (Fig.6) to the elastic process, diagrams with two or four gluons in the t-channel, and we will have to analyse the imaginary part of this amplitude. For the moment, however, we will postpone this question, and in this section we shall consider the space-time structure of the scattering amplitude of this larger class of diagrams.

Counting first powers of α_s and $\ln s$ and comparing with the single ladder, leading $\ln s$ approximation, we have lost two powers of $\ln s$. A consistent QCD analysis requires to study *all* contributions which contribute to this level of accuracy, i.e. we are not allowed to simply limit ourselves to diagrams with two-ladder exchange but have to include much more general classes. Generally speaking, it is expected that they can be divided into two groups. The first one preserves the one-ladder structure but introduces corrections to the BFKL kernel; we expect that will have the same space-time structure as the BFKL ladders itself. The second group of corrections, for which Fig.6a presents a simple example, goes beyond the one-ladder structure and contains both the t-channel iterations of the two-ladder states and the enhanced diagrams (single-ladder state between the coupling to the external particle and the two-ladder states). An example is shown in Fig.6b. These contributions are expected to be of particular relevance for the unitarization of the BFKL Pomeron. In this paper we will restrict ourselves to this latter class of corrections. As we shall see they contain new elements of the space time picture.

As to the four gluon state, it is important to note that the interactions between the four gluons can be arranged in two different ways. Either we can group the pairwise interactions into ladders (e.g. between the lines (12) and (34)). We then have to sum over all “switches“ from one coupling scheme to another (e.g. from (12)(34) to (13)(24)) and over all iterations in the t-

channel. Any such switch can also be viewed as an interaction between two ladders. Alternatively, we could reorder the rungs in the four gluon state in such way that we obtain a geometric series of the kernel $\sum_{ij} K_{ij}$ where the sum extends over all pairs (ij) of gluon lines. It is easy to see that both ways of summing over all rungs lead to the same result. For most of our discussion it will be more convenient to adopt the first method of summation, i.e. to speak about ‘ladders’ and their ‘interactions’.

3.1 Two-Ladder Exchange

Let us organize our analysis in several steps. For simplicity, we first return to scalar field theory. We begin with a two ladder diagram and investigate the coupling of the ladders to the incoming particle. We will show that the leading log contributions comes only from those graphs where one of the reggeons can be put inside the other one (Fig.7a,maximal nested structure) [12]. The diagrams that we are going to analyse are illustrated in Fig.7a and b. As before, in order to get the maximum number of the logarithms one has to order the ‘sizes’ of the reggeons. Let us compare the diagrams Fig.7a and 7b. For the graph 7a it is enough to choose the $\alpha' \gg \alpha''$ and there will be no any problem with the integrations over the β -variables. One can close the contour of the β_R (the momentum fraction transfered through the reggeon as a whole) on the pole $1/q_1^2$, the β'' contour - as usual, on the pole $1/q_2^2$ and then the β' - on the pole $1/q_3^2$. In the case of the graph Fig.7b the situation is quite different. After the β_R integration here we get the two poles (q_2 and q_3) with the largest $\alpha_2 \simeq \alpha_3 \simeq 1$ in the lower half plane of the β'' integral. The leading contributions coming from this poles cancel each other⁴ and finally the graph 7b does not gives the leading logs. From the space-time point of view it is evident. The life-time of the partons $\tau' \gg \tau''$ (at $\alpha' \gg \alpha''$) does not satisfy the required time ordering condition. The parton α'' in Fig.7b should be absorbed after the parton α' , but its life-time is too small to provide this. Thus the configuration shown in Fig.7b does not contribute.

If we choose the wrong ordering $\alpha' \ll \alpha''$ (i.e. the time-live $\tau' \ll \tau''$ we lose the leading log also in Fig.7a. Now for the β_R -integration the two leading poles (with largest values of the α -variables) will both lie in the lower half plane of the β_R plane. Thus we have show that the time interval occupied by the upper parton of the external reggeon $\tau' \propto \alpha'$ should be much larger than the value of $\tau'' \propto \alpha''$, which corresponds to the inner reggeon. This properties of the two reggeon cut kinematics comes originally from the famous S.Mandestam paper[4] and was discussed with respect to QCD in [8].

It should be noted that only the life-time of the top level partons in each reggeon ladder of Fig.7a have to be strongly ordered. About the other partons which are not so close to the vertex of the two reggeon emission we can only say that the values of α'_i and α''_i are ordered in each reggeon separately

$$0 \ll \alpha'_n \ll \dots \ll \alpha'_2 \ll \alpha'_1 \ll 1.$$

$$0 \ll \alpha''_n \ll \dots \ll \alpha''_2 \ll \alpha''_1 \ll 1.$$

⁴As the two poles with the largest α are enough to provide the convergence of the β integral, one can omit the β in all the other propagators (with the smaller value of α_i) and then closing the contour of integration in the upper half plane (where there are no any singularities now) get the zero.

and there are no any special relations between the time-life (i.e. the values of α'_i and α_i'') of the partons from different reggeon.

At the lower end of the diagram Fig.7a the picture is exactly the same. The best way to see it is to go to the beam particle (Q) rest frame. In this frame the lowest partons have the largest time-life $\tau_{n-1} \propto \beta_n$, and we have to put $\beta'_n \gg \beta_n''$ or $\beta_n'' \gg \beta'_n$. As it was mentioned above the ordering at the bottom does not correlate with the ordering at the top of the graph and any combination of the regions $\beta'_n \gg \beta_n''$ or $\beta_n'' \gg \beta'_n$ and $\alpha' \gg \alpha''$ or $\alpha'' \gg \alpha'$ do gives the leading log contribution. Of course each time one has to draw the Feynman diagram in such a way that the reggeon with the largest α would be the external one at the top and - one with the largest β - at the bottom of the diagram.

The generalization to QCD is straightforward. The discussion given in this section applies directly to the case where both gluon ladders couple to the same quark line. But since we have to sum over all possibilities of attaching the ladders to the quark antiquark pair, we also have to say a few words about the other configurations. As a rule we state that, in order to contribute to the leading logarithmic approximation, the life time of the first rung of one ladder has to be larger than that of the second ladder. In particular, this implies that in the contribution where one ladder couples to the quark, the other to the antiquark, only those time orderings survive where one ladder “is fully contained“ inside the other.

3.2 The Space Time Picture of a Two-Pomeron Interaction

As the next element of our general class of diagrams illustrated in Fig.6b we analyse the space-time structure of the interaction between two ladders (Fig.7c - f). For simplicity we ignore the complications due to the reggeization of the gluon and the complex structure BFKL rung, and consider the scalar case. Figs.7c,d, and f are examples of switches from one way of pairing to another. For example, starting in Fig.7d from below, we first have the pairing (12)(34), then, after one rung between line 1 and 3, the pairing (14)(23). Equivalently, one might say that the ladders (12) and (34) interact with each other and then continue as ladders (14)(23). The switch from the lower pair of ladders to the upper ones can, alternatively, be viewed as the interaction between two ladders, i.e. as a $2 \rightarrow 2$ Pomeron vertex. Cutting Fig.7d by a vertical line between the second and the third t-channel line we obtain intermediate states with double multiplicities in the upper half. The main result to be derived in the following is that, for diagrams of this type, the second and third t-channel lines must have *changes in the direction of time*. (the observation that partons may have negative fractions of momentum has also been mentioned in [9]). To illustrate this statement, let us remind that in two noninteracting ladders (14) and (23) (Fig.7a) along lines 1 and 2 the time arrows always point downwards, along llines 3 and 4 upwards. Obviously, rungs always connect t-channel lines with opposite time directions. The new feature to be explained in the following is that, as soon as we try to introduce rungs between lines 1 and 2 (or 3 and 4), the time flow along lines 2 and 3 must change its direction.

Before we discuss this feature of Fig.7d in more detail, let us first show that not all switches lead to a nonzero contribution, even if we allow for changes in the time direction. For example, one might try to draw a configuration with zero density in the central region (Fig.7c). In the be-

ginning, let us consider the situation where we have the usual ordering along the second t-channel line (i.e. the line in Fig.7c which carries α_2 should be drawn with the arrow in the opposite direction). Then one sees easily that the t-channel gluons 1 and 2 (or 3 and 4) cannot interact with each other. Indeed, in order to receive the leading log in the α_i integration one has to close the β_i contour around the pole $1/q_i^2 = 1/(\alpha_i\beta_i s - \mathbf{q}_i^2)$ with the largest α in the whole β_i loop (see Fig.1a). This pole gives us $1/\alpha_i s$ and then the integral $\int_{\mathbf{k}^2/s}^1 \frac{sd\alpha_i}{s\alpha_i} \propto \ln s$. The contributions of the $\alpha_j\beta_i s$ ($j > i$) terms in all other propagators, say, $(1/k_{i+1}^2, 1/k'_{i+1}{}^2, \dots)$ are small in this case and we may neglect the $\alpha_{i+1}\beta_i s = (\mathbf{q}_i^2 + m^2) \frac{\alpha_{i+1}}{\alpha_i}$ term in comparison with $q_{i,t}^2$, because of the α ordering ($\alpha_{i+1} \ll \alpha_i$). So, if the value of α' (dashed line in Fig.7c) is smaller than α_3 we lose the log in the α_3 loop. The term $\alpha_3\beta' s$ becomes the dominant one in the propagator $1/k_3^2$, and the integral over α_3 looks as $\int d\alpha_3/\alpha_3^2$. If, on the other hand we change in Fig.7c the direction of the line α_2 (as drawn in Fig.7c), we still get zero. Namely, if $\alpha' \gg \alpha_3$ then $\alpha_2 \simeq -\alpha'$ becomes negative. For the β_2 integration we then have two poles in the lower half plane, and they cancel each other ⁵.

Now let us return to Fig.7d and show that by changing the arrows for the two vertical gluon lines we obtain a nonvanishing contribution. As before the arrows indicate the sign of the α_i variable (i.e. the direction of time) and the vertical position of each horizontal line reflects the α ordering ($\alpha_1 \gg \alpha_2 \gg \alpha_3 \gg \dots$). The dashed lines show the structure of the β_i loops, while the doubled (dashed) part of this lines mark the propagators with the largest α in each β loop. Points, where the arrow changes its direction (sign of α) are marked by open circles. Almost all the integrations in the graph Fig.7d look as usual. For example, the β_4 integration picks up the pole $1/q_4^2$, the β_5 integration the pole $1/q_5^2$, β_0 the pole $1/q_0^2$ and so on. Two exceptions are the β_2 and β_3 loops, where pairs of poles ($1/q_2^2$ and $1/k_3'^2$ for β_2 , and $1/q_3^2$ and $1/k_5^2$ for β_3) lie in the lower complex halfplane. To be sure that these pairs of poles do not cancel we have to choose $\alpha_{(k)3} \approx \alpha_3 \gg \alpha_{(k')3} \approx \alpha_4$ and $\alpha_4 \gg \alpha_5$. The convergence of the β_2 and β_3 integrations are guaranteed by the poles $1/q_2^2, 1/k_3^2$ and $1/q_3^2, 1/k_4^2$, resp., which are located in opposite half planes. The contributions of β_2 and β_3 terms in all other propagators are negligible.

The general condition which, for example in Fig.7d, leads to the nonvanishing contribution is the following: below the vertices marked by a circle on line 2 and 3 we have to change the signs of the α variables, i.e. the direction of time. Namely, the α ordering has to fulfill the requirement that, for a given β -loop, the α -value on the vertical line opposite to the marked vertex is much larger than in the vertical line below the marked vertex: $\alpha_3 \gg \alpha_3'$. This is the formal way to check whether a given time ordering will lead to a nonzero contribution.

A more intuitive way to distinguish between vanishing and contributing time orderings is the following: in order to have a nonvanishing contribution it must be possible to draw the space time diagram (see, for example, Fig.7e) in such a way that one of the two ladders is fully inside the other. In other words, emission (and absorption) of the first rung of the outer ladder must happen before (and after) the emission (and absorption) of the rung of the inner ladder. In Fig.7e we show the space time picture of Fig.7d: obviously we can move the marked vertices until one ladder is totally inside the other. In Fig.7f we present another example, with the crossing symmetry (with

⁵This two poles with the largest α ($\alpha = \alpha_1$ or $\alpha = -\alpha'$ provide the convergence of the β_2 integration in the region $|\beta_2| \sim \mathbf{q}_i^2/\alpha' s$. Therefore we can omit the β_2 terms in other propagators (where its contribution is small) and then close the contour in the upper half plane where there are no any singularities now. Thus the β_2 integration gives the zero result.

respect to the gluons 2 and 3) amplitude.

3.3 The Full Diagram

Let us finally collect our results and attempt to give a space-time description of the scattering amplitude of a general diagram Fig.6a or b.. For simplicity we restrict ourselves to the reference frame where the photon is fast and the proton is at rest. Beginning at the upper end where the photon dissociates into the quark- antiquark pair, we consider the case where two gluons are radiated from (and later on reabsorbed by) the quark pair. What we have shown is that, depending on the coupling of the four gluon lines to the quark pair, only selected time orderings are relevant, For example, if all gluon couple to the same quark line only those configurations survive where the first s-channel gluon produced from the first t-channel gluon has to be reabsorbed last, and the decay products of the second gluon have to be reabsorbed first. In other words, the “inner rungs“ must be fully contained inside the “outer rung“. This restriction holds only for the first rung in each ladder. After this, the formation of ladders between lines 1 and 4, and lines 2 and 3 may continue: each reggeon then continues its own cascade in such a way that the life times of the rungs is getting shorter and shorter. As a part of this requirement, a rung can connect only lines with opposite time direction. After the first rung in each ladder, there is no further correlation in time between the rungs of the first and the second reggeon.

After a few steps it may happen that the two ladders interact, e.g. a rung from 1 goes to 3 or from 2 to 4. This requires no change in the time direction. However, if a rung emitted from 1 wants to be absorbed by 2, line 2 has to change its direction. The example of Fig.7c demonstrates that even with this change of the time direction we may get zero. As stated at the end of section 3.2, in order to have a nonzero contribution we have to be able to draw the space time structure in such a way that the new ladders (12) and (34) can be put one inside the other. The formal way is, again, to check that the leading poles of the β integrals (i.e. the ones with largest α -values) always lie on different sides of the real axis. Fig.8 shows two more examples, illustrating the space time structure of more complex configurations. Alternatively, we can also have the situation that initially only one gluon is emitted from the quark pair (and later absorbed again). In this case, below the quark pair first a single reggeon ladder develops, as described in the beginning of this paper. After some time, one gluon rung emits and absorbs an extra gluon: this four gluon system now develops in the same way as described in the previous paragraph. In particular, initially the two ladders starting at the gluon rung have to be maximally nested again.

Finally there are less symmetric configurations: at the top the one of the two quarks produces a gluon, and the rungs connected to this gluon may end at two different lines. In this way two ladders develop which have one line in common. After a while, there may be a rung between line 2 and 3: in order that such a rung has the correct time structure, line 2 has to change its time direction.

3.4 A Remark on the Diffractive Dissociation

It may be worthwhile to explore in more detail why certain time orderings do not contribute to the high energy behaviour of the scattering amplitude. In many cases, the formal way of eliminating a particular time ordering is the cancellation of poles in β -integrals. This is nothing else but saying that different contributions to the imaginary part of the scattering amplitude cancel against each other. In the following, we illustrate this cancellation for a case of particular interest, the AFS diagram shown in Fig.9a and b. The reason why this configuration plays a special role is the following. From the discussion of the previous section it follows that this configuration does not contribute to the scattering amplitude (it is not maximal-nested). On the other hand, the contribution to the imaginary part which follows from putting the two-particle intermediate state on mass-shell (Fig.9c), represents the square of “elastic scattering “. So, at first sight it seems mysterious how the (very important) elastic cross section (Fig.9c) disappears inside the scattering amplitude of Fig.9b. The resolution of this somewhat puzzling situation follows from the old arguments of Amati, Fubini, Stangellini [3] and Mandelstam [4].

Let us first review the argument for the simple scalar $\lambda\phi^3$ theory; later on we shall demonstrate that QCD works the same way. Beginning with the space time picture in Fig.9b it is quite obvious why, in the scattering amplitude, this configuration cannot be realized: on the one hand, the longitudinal distance between the partons n' and n" should be larger than the life time $\tau_1 \sim E_1/\mathbf{q}_t^2$ of the rungs at the top. On the other hand, at high energies this separation will be much larger than the size of the target which characterizes the separation between the points p' and p" at the bottom of Fig.9b. Next, looking into the high energy formula of this diagram one finds that it vanishes since for the central β -integral the three leading poles (with the largest α_i) lie all on the same side of the integration contour: closing the contour in the opposite half plane gives zero. Equivalently, the sum of the three poles adds up to zero. This cancellation can also be seen if we decompose the imaginary part of the diagram. Three contributions belonging to low multiplicity final states are illustrated in Fig.9c and d (not shown is the conjugate of Fig.9d), and they can be shown to cancel each other. The first contribution (Fig.9c) is positive, and it describes the elastic cross section. The two other terms (Fig.9d and its conjugate) are negative, since the virtuality q_0^2 is positive while the propagator $1/k'^2$ in Fig.9d is negative.

In this way, in $\lambda\phi^3$ theory, the planar diagram of Fig.9a does not contribute to the elastic scattering amplitude. Nevertheless, elastic and diffractive dissociation intermediate state exist and give a nonzero contributions. Their sum, however, adds up to zero. In QCD we have the same pattern of cancellations, but - mainly because of the vector nature of the gluon - some important details are different. First we have to remember that, when we draw reggeon diagrams with BFKL interaction kernels, we are, in fact, summing over larger classes of Feynman diagrams and combining them into reggeons and “effective“ nonlocal vertices. For example, in a convenient axial gauge $p'_\mu A^\mu$ the BFKL effective gluon production vertex is obtained from the sum of three Feynman diagrams shown in Fig.10a. Therefore, in order to demonstrate the AFS cancellation in Fig.9a (now with reggeized gluon lines in the t-channel, and BFKL vertices for the rungs), we need to decompose the BFKL kernels on both sides. This is illustrated in Fig.10b where we decompose the upper rung inside the left hand ladder. In Fig.10c we draw the corresponding discontinuities which, according to the AFS mechanism, are needed in order to cancel the elastic intermediate states.

In order to show in more detail that in QCD this cancellation really works in the same way as

in the scalar theory, a few comments are in place. First, since the triple gluon vertex V_3 in the first diagram Fig.10b has a nontrivial dependence upon the virtualities of its external lines, we have to check that Fig.10c really has the same expression. Working in the axial gauge $p'_\mu A^\mu$ the gluon propagator takes the form

$$\frac{d_{\mu\nu}(q^2)}{q^2}, \quad d_{\mu\nu}(q^2) = g_{\mu\nu} - \frac{q_\mu p'_\nu + p'_\mu q_\nu}{qp'} \quad (6)$$

with $d_{\mu\nu}p'^\mu = 0$ and $d_{\mu\nu}q^\nu \simeq -\frac{qt_\mu}{\alpha_q}$. As it is well-known [10], in the high energy limit a t-channel gluon is dominated by the longitudinal “nonsense“ polarization, i.e. $\sum_\lambda e_\mu^\lambda e_\nu^\lambda \approx p'_\mu q'_\nu / (q'p')$. In our gauge it means that at the upper end the polarization vector e_μ of the gluon is p'_μ , whereas at the lower end one contracts with q'_ν : $d_{\mu\nu}(k)q'^\mu = -\frac{2k_{t\nu}}{\alpha_k s}$. Now the elementary vertices shown in Fig.11 take the form: $\Gamma_a = -2k_{t\sigma}$, $\Gamma_b = \alpha_i \delta_{\sigma\sigma'}$, $\Gamma_c = -\frac{2q_{t\sigma}}{\alpha_q}$, and with the help of $k^2 = -\mathbf{k}_t^2$, $q_s^2 = \mathbf{q}_t^2 / \alpha_q$ it is easy to see that the three graphs in Fig.10b sum up to the effective BFKL vertex:

$$-\frac{2k_{t\sigma}}{k^2} - \frac{2q_{t\sigma}}{\alpha_q q_s^2} = \frac{2}{\mathbf{k}^2 \mathbf{q}^2} (\mathbf{q}^2 k_{t\sigma} - \mathbf{k}^2 q_{t\sigma}). \quad (7)$$

Applying the same expressions for the vertices (with $q_s^2 = \mathbf{q}^2 / \alpha_q$) to the first graph in Fig.10c, we see that in fact it reproduces the first term of the BFKL vertex, while the second and the third graphs in Fig.10c reproduce the last term of eq.(7).

Another point to be mentioned is that the left hand part of the second diagram in Fig.10b, as a Feynman diagram, does not contribute to the leading logarithmic approximation. The two contributions coming from the β poles of the $1/q_s^2$ and the $1/q_s'^2$ propagators cancel each other (i.e. the AFS cancellation repeats itself inside a single ladder). This cancellation reflects the wrong space time structure of this diagram: the life time of the gluon with momentum q is larger than the separation between the points 2 and 1. On the other hand, when computing the BFKL ladder with a fixed number of gluons in the final state, the pole of the q_s line is taken into account in order to produce the BFKL vertex on the rhs of the ladder, whereas the pole of the q'_s line goes into the reggeization of the upper left t-channel gluon.

Both the AFS cancellation and the cancellation of poles in the second diagram of Fig.10b are examples illustrating that, at high energies, a Feynman amplitude may give a zero contribution to the scattering amplitude, but at the same time may contain nonzero contributions to partial cross section. Other examples of this phenomenon can be found in [13].

4 The AGK Cutting Rules for the Exchange of Two Regge Poles

So far we have tried to develop a space-time picture of the scattering amplitude for the process $\gamma^* + p \rightarrow \gamma^* + p$, generalizing from the one-ladder approximation to diagrams with up to four gluons in the t-channel (in the s-channel, as we have demonstrated, this corresponds to higher order partonic interactions). Now we turn to the question of intermediate states, in particular the contribution of the diffractive dissociation. As we have said before, this question has to be answered by an analysis of the contributions to the imaginary part (or energy discontinuity), i.e. by a

study of the unitarity content of our diagrams. Here we will make use of the AGK cutting rules [2].

It may be helpful to first briefly review the content of these rules. For a two-reggeon exchange (Fig.12) the scattering amplitude is of the form [14]:

$$T = -is \int d\Omega_2 N(i\xi_{\alpha_1} s^{\alpha_1-1})(i\xi_{\alpha_2} s^{\alpha_2-1})N \quad (8)$$

Here the N 's denote the (real-valued) partial waves above and below the two reggeons in Fig.9 (which by themselves may contain Regge cut singularities), α_1 and α_2 are the reggeon trajectory functions, and the signature factors are

$$\xi_\alpha = \frac{e^{i\pi\alpha} \pm 1}{\sin \pi\alpha} \quad (9)$$

The detailed form of the phase space integral in eq.(8) is not of importance for our present discussion and can be found in [2]; in fact, we only need the phase structure of (8):

$$T \sim -i(i\xi_1)(i\xi_2) \quad (10)$$

From (8) we find

$$2ImT = 2(Re\xi_1 Re\xi_2 - Im\xi_1 Im\xi_2). \quad (11)$$

Now the AGK rules state that the same result can be obtained by summing separate contributions to the imaginary part. Namely, the diffractive cut σ_0 with zero multiplicity in the central region (Fig.12, the cut runs between the two reggeons), the multiperipheral cut σ_1 with single multiplicity (cutting one of the two reggeons), and the double multiperipheral cut σ_2 with double multiplicity (cutting simultaneously both reggeons) give

$$\begin{aligned} \sigma_0 &= 2(Re\xi_1 Re\xi_2 + Im\xi_1 Im\xi_2), \\ \sigma_1 &= -8Im\xi_1 Im\xi_2 \\ \sigma_2 &= 4Im\xi_1 Im\xi_2, \end{aligned} \quad (12)$$

resp. (the factors 2, 4, and 8 count the different possibilities of interchanging reggeon 1 and 2). Taking the sum of these cuts, $\Sigma\sigma = \sigma_0 + \sigma_1 + \sigma_2$, we obtain, in fact, the result (11). In [2] one also finds a generalization to an arbitrary number of reggeons.

The most interesting case is the two Pomeron exchange (even signature with intercept close to one). Here we can neglect the real part of the signature factors, and for the ratios of the various cuts we obtain:

$$\sigma_0 : \sigma_1 : \sigma_2 : \Sigma\sigma = 1 : -4 : 2 : -1 \quad (13)$$

To clarify the physical meaning of the relation (13) we will discuss the scattering of a hadron h on a deuteron target. In the impulse approximation the cross section is simply $\sigma^{(0)}(hd) = \sigma(hp) + \sigma(hn)$. However, for some part of the time the impact parameters b_t of the proton and neutron inside the deuteron may coincide and they shade each other. Let us assume, for simplicity, that the nucleons inside the deuteron are the grey disks with constant opacity $\xi < 1$ ($\xi = 1$ corresponds to a black

disk) and area S , and put $b_{t,p} = b_{t,n} = 0$. Then the inelastic cross section for the scattering of the hadron h on a single nucleon is simply $S\xi$. In this reaction, the final state has single density of the secondary hadrons. Due to the optical theorem it is easy to obtain the elastic cross. The imaginary part of the forward scattering amplitude is given by:

$$2\text{Im}f_{el}(b) = |f_{inel}(b)|^2 + |f_{el}(b)|^2 \quad (14)$$

Assuming that $\xi \ll 1$, and making use of the fact that at high energies the scattering amplitude with positive signature amplitude is imaginary, we get $\sigma_{el}(hN) = S(\xi/2)^2$. Thus the sum of cross sections is:

$$\sigma(hp) + \sigma(hn) = 2(\sigma_{inel} + \sigma_{el}) = 2S\xi + S\xi^2/2 \quad (15)$$

This is the impulse approximation result.

The corrections to this result come from different sources:

- i) near the second target(nucleon) the initial flow of the beam hadrons has become smaller by a factor $1 - \xi$, due to the absorption on the first target. This gives a correction $\Delta\sigma_{1(i)} = -S\xi^2$.
- ii) after the interaction with the first target with the probability ξ the next inelastic collision with the second nucleon takes place, leading to the doubled multiplicity of the secondaries instead of the single one. This leads to a further decrease of the cross section σ_1 by $\Delta\sigma_{1(ii)} = -S\xi^2$. Both corrections affect the final states with single multiplicity. Their sum is $\Delta\sigma_1 = \Delta\sigma_{1(i)} + \Delta\sigma_{1(ii)} = -2S\xi^2$.
- iii) At the same time we obtain for the double multiplicity final state $\Delta\sigma_2 = +S\xi^2$.
- iv) Finally, for the elastic scattering cross section on a target with the two overlapping grey disks one should use for the inelastic cross section in (14) $2S\xi$ which leads to $\sigma_{el} = S\xi^2$, i.e. a correction to (15) of the form $\Delta\sigma_{el} = \Delta\sigma_0 = S\xi^2/2$. Putting all these corrections together we obtain

$$\Delta\sigma_0 : \Delta\sigma_1 : \Delta\sigma_2 = 1 : -4 : 2 \quad (16)$$

quite in agreement with the AGK rules[2].

The physical interpretation of these corrections is, indeed, the same as suggested by the AGK rules. Namely, starting with the correction $\Delta\sigma_2$, which belongs to the final states with double multiplicity, it correspond to cutting both ladders simultaneously (σ_2 in (13)). The space-time structure is illustrated in Fig.13a. The two contributions to $\Delta\sigma_1$ have single density final states, i.e. they cut only one of the two ladders (σ_1 in (13)) (Fig.13b). They describe the screening corrections to the single multiplicity contribution, due to the rescattering of the hadron h on the "second" target. Finally, the correction $\Delta\sigma_0$ corresponds to Fig.13c; it corresponds to the diffractive cut (σ_0 in (13)). It should be stressed that we detect the final hadrons far away and long time after from the collision. Therefore it is possible to follow the rescattering in the single amplitude in Fig.13b or c: there is enough time to create and than to recollect the whole ladder which describe the reggeon exchange before the secondary hadrons reach our detector.

Finally let us consider a two reggeon exchange amplitude in which the reggeons have odd signature with intercept close to one. This case will become important when, in the following section, we have to deal with the reggeizing gluon in QCD. In contrast to the even signature case, the signature factor now is approximately real, and from (12) one sees that the diffractive cut σ_0 dominates. So the AGK rules lead to a quite different result. Instead of (13), we now have

$$\sigma_0 : \sigma_1 : \sigma_2 : \Sigma\sigma = 1 : 0 : 0 : 1 \quad (17)$$

In other words, cutting an odd signature reggeon gives a subdominant contribution compared to the uncut reggeon. In QCD, this means that cutting a reggeizing gluon brings us down by a power of α_s (i.e. we are losing one power of $\ln s$), and it is clear that the leading-log approximation, the BFKL Pomeron ladder, is entirely due to the cut which runs in the middle of the ladder and never touches a reggeized gluon. It should, however, be noted that the “old“ AGK rules (13) remain valid also for the odd signature reggeons, if we restrict ourselves to the (nonleading) imaginary parts.

5 The AGK rules in QCD

Now we are ready to discuss the cutting rules for the diagrams with four t-channel gluons in QCD (left half of Fig.14a). The simplest way to confront these QCD diagrams with the AGK rules is the following. We first redraw the sum of all diagrams as reggeon diagrams with reggeized gluon propagators and BFKL kernels. This amounts to combining sums of Feynman diagrams in a special way. Next we consider the t-discontinuity across the four reggeon state. Loosely speaking, this is equivalent to selecting a four gluon t-channel state in the center of the diagrams and then summing independently above and below this state over all t-channel iterations. In other words, instead of the scattering amplitude itself we consider its t-channel discontinuity across the four - reggeon cut (Fig.14a). What appears above and below the selected four reggeon state are - almost- the t-channel partial waves with four gluons in the t-channel. Pairs of two reggeized gluons form bound states, in particular Pomerons with vacuum quantum numbers, and we then will be able to compare Fig.14a with Fig.12 and eq.(8). Our goal is the analysis of the different contributions to the discontinuity in s , i.e. we will have to analyse how the different s-cut lines pass the selected four gluon state.

From our previous discussions it follows that in our analysis of the four reggeon intermediate state we cannot avoid to discuss also the odd signature reggeon. Namely, as we have argued in section 3, in the diagrams of Fig.14a we are now down by two powers of α_s compared to the leading one-ladder approximation, and at this level we expect not only to see the two-Pomeron cut but also contributions with two cut odd signature reggeons, e.g. the double multiperipheral cut of the BFKL Pomeron (cf. the discussion at the end of the previous section). Consequently it is to be expected that the diagrams in Fig.14a contain contributions other than the double exchange of two even-signature reggeon ladders to which the AGK rules (13) apply. The odd-signature contributions should be removed (and considered separately) before we can compare with the AGK rules. In order to isolate these contributions we have to concentrate on those configurations where the two ladders are in an octet state, i.e. we have to adress the bootstrap problem which we have mentioned already before.

The simplest example for the bootstrap mechanism in QCD is given by the BFKL ladder diagrams. They represent the leading logarithmic approximation for the imaginary part of the elastic scattering amplitude. For the color singlet exchange case this provides the leading approximation for the amplitude. For the octet exchange, however, the amplitude which is given by the exchange of a single reggeized gluon, is real-valued, and the imaginary part is down by one power of α_s . In order to match the leading real part, the imaginary-valued BFKL ladders, when projected onto the color octet state, must coincide with the single reggeized gluon exchange. This is, in fact, the case: the “sum of the ladders is identical with the single reggeized gluon“. This identity is referred to as

the bootstrap property.

For amplitudes with more than two gluons in the t-channel one meets similar identities. For example, from the LLA analysis given in [13] one obtains for the four gluon amplitude N_4 in Fig.14a above the four-reggeon state that, whenever two neighbouring gluons are in the antisymmetric color octet state with odd signature, the two gluons “collapse“ into a single reggeized gluon. These contributions are then simple BFKL ladders with a splitting of the reggeized gluons into two (or even three) gluons at the lower end. Applying this result to the amplitudes in Fig.14a above and below the four gluon state, one easily sees that, for example, there will be a contribution where lines 1 and 2 and lines 3 and 4 “collapse“ into single odd-signature gluons. Obviously, for these contributions the AGK rules have to be interpreted differently from the even signature (as we have discussed in the previous section). In [13] a complete analysis of the four gluon amplitude has been performed, and it has been shown that the four gluon amplitude which consists of the diagrams illustrated in Fig.14a can be written as a sum (Fig.14b) of reggeizing pieces and an “irreducible“ remainder (Fig.14c) which is free from any odd-signature admixtures. In the following we will first consider this latter part. At the end of this section we shall return to the reggeizing contributions.

After having isolated and removed all those states where ladders “collapse“ into reggeized gluons, the remaining “irreducible“ piece has a very special structure. First of all, it contains only “enhanced“ diagrams (Fig.14c). This means that in this irreducible part the four-gluon state does not couple directly to the external photon. For it has been shown in [13] that all diagrams where three or four gluons couple directly to the quark loop belong to the reggeizing contributions of Fig.14b. What remains for the irreducible piece Fig.14c are BFKL ladders between the quark loop and the transition vertex: two-gluons \rightarrow four gluons (this is a new element in the BFKL dynamics. It has been derived and discussed in [13, 15]). Below this vertex the four gluon state starts. An important property of the transition vertex is its symmetry (both in momentum and color) under the exchange of any two of the four outgoing gluons. The subsequent two-body interactions between the four gluons preserve this symmetry, and consequently the four gluon state remains completely symmetric. Finally, as discussed at the end of section 3, we re-group the interactions inside the four reggeon state into ladders - e.g. first all pairwise interactions inside the subsystems (12) and (34), then for the pairing (13), (24) and so on. Because of the symmetry, the ladders have always even signature, and the amplitude is completely symmetric if we interchange any pair of lines. It is important to keep in mind that the ladders are not restricted to the color singlet configuration, i.e. they can be also in the symmetric 8 or 27-representation.

Putting now together these irreducible pieces from above and from below, it is easy to compare the different ways of cutting these diagrams. First we note that a vertical cut across the diagram in Fig.14c does not alter its (absolute) value: when the line intersect a horizontal (s-channel) gluon, the discontinuity $2\pi\delta(q_i^2)$ is the same as the pole contribution (we have argued before that all s-channel gluons are on the mass shell). This statement applies to both the rungs inside the four gluon state and the $2 \rightarrow 4$ transition vertex. In particular, the transition vertex does not depend upon if and where we draw a cutting line. On the other hand, if we intersect a vertical gluon line we lose one (or more) power of $\ln s$. Therefore, in the following all cuts will run between t-channel gluon lines. Let us pick, inside the four gluon system, a two-ladder state, and let the discontinuity line run between the gluon lines “2“ and “3“ (Fig.15a). If the rungs above and below belong to the pairing (12)(34), we have the diffractive cut which comes with the weight $+(\frac{1}{2!})^2$ (this includes the

statistics factors for the two-gluon t-channel states on both sides of the cutting line). If the rungs belong to the assignment (13)(24) or (14)(23), we obtain the double multiperipheral cut (Fig.15c) with weight $+2(\frac{1}{2!})^2$. Next let the discontinuity line pass between lines “1“ and “2“ (Fig.15b). Now all pairings belong to the single multiperipheral cut, and together they give the weight $-3\frac{1}{3!}$ (the simplest way to understand the negative sign is by looking at a situation where inside the system (234) two of the gluons, say 2 and 3, form an even signature Pomeron state. In this case the Pomeron exchange can be viewed as an absorptive correction to gluon 4, and therefore comes with a relative minus sign). The same contribution is obtained from the discontinuity line between the lines “3“ and “4“. In summary, we have the relative weights

$$\sigma_0 : \sigma_1 : \sigma_2 = +1/4 : -1 : +1/2, \quad (18)$$

which agrees with the AGK cutting rules in eq.(13).

Note that in this argument we did not refer to any color coefficients: all that went into our argument is the complete symmetry of the four gluon state under the exchange of color and momenta of gluon lines. We clearly are allowed to conclude that the AGK rules are satisfied for the two-reggeon states with vacuum color quantum numbers, i.e. Pomerons. But our analysis also shows that Pomeron ladders are not enough: even-signature ladders with nonzero color are present and participate in the AGK rules (for these ladders, the cut between the ladders should no longer be called “diffractive“).

The presence of these color nonsinglet ladders has a very important practical consequence. Since the full set (Fig.14a) of four-reggeon corrections to the scattering amplitude contains also these non-vacuum quantum number two reggeon ladders, a measurement of the diffractive dissociation cannot be used to estimate the size of Fig.14a, i.e. the full unitarity correction. In the diffractive dissociation one measures, at least for sufficiently large rapidity gaps, only the vacuum quantum number ladders on both sides of the cutting line. The diagrams in Fig.14a, on the other hand, also contain color nonzero ladders: their final states are expected to have similar characteristics as the BFKL ladders. In particular, the produced s-channel gluons are color-connected, and the probability for events with a rapidity gap is small.

So far we have concentrated on the two-ladder (four-reggeon) intermediate state in the center of Fig.14a; this was the original form of the AGK relations. Next one could try to trace the discontinuity line above (or below) the four gluon state that we have considered so far. On other words, we now consider Fig.14c and study how a cutting line changes from, e.g., “diffractive“ to “multiperipheral“. Rearranging, inside the four gluon state of Fig.14c, the rungs in terms of ladders, we immediately see that at any switch (i.e. a change of the pairing (ij)(kl) to (ik)(jl)) the nature of a cutting line may change. For example, at the switch (12)(34) \rightarrow (13)(24) the discontinuity line between line “2“ and “3“ changes from “diffractive“ to “multiperipheral“. On the other hand, the line between “1“ and “2“ remains “multiperipheral“. Considering all possibilities, we arrive at the following transition matrix:

<i>from :</i>	σ_0	σ_1	σ_2
<i>to : σ_0</i>	0	0	1/2
σ_1	0	1	0
σ_2	1	0	1/2

(19)

Let us note that this matrix (19) is nontrivial: instead of the usual (1:-4:2) relation we now find that there are no transitions from single to double (or zero) densities cuts, only from single to single, from double to double, double to zero, and from zero to double multiplicity. Furthermore, this matrix conserves the initial AGK ratios (13). Indeed, if at the beginning of the four gluon state we had the relations $\sigma_0 : \sigma_1 : \sigma_2 = 1 : -4 : 2$ then after the $2 \rightarrow 2$ pomeron interaction (which includes the sum of all type of the vertices (14)(23) \leftrightarrow (12)(34), (14)(23) \leftrightarrow (13)(24), (12)(34) \leftrightarrow (13)(24)⁶) we get $2 \cdot \frac{1}{2} : -4 \cdot 1 : (1 \cdot 1 + 2 \cdot \frac{1}{2}) = 1 : -4 : 2$ again. In other words, the vector $(1, -4, 2)^T$ is an eigenvector to the matrix (19). Thus in any rapidity interval the relative contributions of the processes with zero : single : doubled densities of the secondary particles remain 1:-4:2.

Nevertheless, taking into account the pomeron-pomeron interactions we get different two-particle rapidity correlations. As it was shown in [2] and was discussed in more detail in [16] the admixture of the two pomeron cut contribution to the single pomeron (ladder) exchange leads to the nonzero positive correlation in the inclusive two particle distribution:

$$R_2 = \frac{d^2N}{dY_1 dY_2} / \left(\frac{dN}{dY_1} \frac{dN}{dY_2} \right) - 1 > 0 \quad (20)$$

(here N is the number of particles at the given rapidity Y). This correlation is the long range one. The value of R_2 (due to the pomeron cut with $\alpha_P(0) = 1$) is constant (i.e. does not depend on $\Delta Y = Y_1 - Y_2$ in the whole rapidity range occupied by the pomeron cut). Now after the ladder-ladder interactions the correlation $R_2(\Delta Y)$ becomes smaller as with the probability equal to 1/2 (see table(19)) the double multiperipheral cut turns into the diffractive one. The value of R_2 is still positive, but falls down with ΔY . The characteristic correlation length Δ (R_2 becomes small at $|\Delta Y| < \Delta$) reflects the average distance between the $2 \rightarrow 2$ pomeron vertices.

Let us finally return to the reggeizing contributions (Fig.14b) which we have left out so far. Starting point is the decomposition illustrated in Fig.14b, and we have to insert these reggeizing pieces above (and below) the four gluon state in Fig.14a. The sum in the second line of Fig.14b includes color octet odd signature reggeons (i.e. the reggeized gluon), but also color octet even signature reggeons as well as color singlet even signature reggeons. Moreover, the reggeons may split into two or three gluon propagators. Finally, we have to sum over permutations of the lower lines. The complete formula can be found in [13]. For our discussion we need to mention only one of its most important properties, namely the symmetry under the exchange of gluon lines. For the even-signature reggeons splitting into two gluons, the sum of all reggeizing terms is completely symmetric under the simultaneous exchange of momenta and color indices. In an obvious notation, the sum can be written as (12)(34)+(13)(24)+(14)(23) where the labels refer to both color and momentum assignment. Consequently, we have a complete symmetry under the exchange of gluon lines. For the odd-signature reggeons (the reggeized gluon), we have a mixed symmetry: we again sum over all pairings: i.e. (12)(34)+(13)(24)+(14)(23), but for each pairing (ij)(kl) we now have antisymmetry under the exchange of i and j or k and l. For the terms where one of the two reggeons splits into three gluons, it carries the gluon quantum numbers, and we have the sum 1(234)+2(134)+(124)3+(123)4. So we have symmetry under the exchange of any two gluons. For each term i(jkl), however, the subsystem (jkl) has a more complex structure. Either the pair (jk) or the pair (kl) are in a state with definite color and signature, such that the system (jkl) forms an odd signature color octet.

⁶The contributions of each of them are equal to each other[11]

When inserting these reggeizing pieces into Fig.14a, we generally have three contributions: reggeizing pieces from above and below, reggeizing pieces only above or only below the four-reggeon state. The two latter contributions again describe a transition from the two-reggeon state to a four reggeon state; because of the symmetry properties, the AGK rules work the same way as discussed above (note that the odd signature reggeons drop out: since the four gluon state from below is completely symmetric, it cannot couple to an odd signature reggeon). So all we have to discuss is the first combination, the reggeizing terms from above and below.

The sum of all these terms, once more, splits into several categories. First we have the “diagonal terms“ (Fig.16a), where the reggeons from above and below match. These terms have the structure of eq.(8), and it is straightforward to discuss the AGK rules. For the even-signature reggeons from above and below the counting is exactly the same as for the two-reggeon ladders above: we simply replace “cut ladder“ by “cut reggeon“ and, with the same statistic factors, reproduce the weights of the imaginary parts in eq.(13). Only for the odd signature reggeons (the gluon) the counting is somewhat different. First the contributions where both reggeons split into two gluons. As we have discussed at the end of section 4, for an odd signature reggeon the real part dominates, and according to (8) the diffractive cut with zero multiplicity dominates. This leading contribution is given by the BFKL Pomeron. In the nonleading QCD diagrams that we are presently studying we expect to see the (subleading) imaginary parts of the gluons: with the symmetry properties mentioned above it is easy to see that, in fact, they come in accordance with (8). Finally the contributions where the reggeized gluon splits into three gluons. Let us consider the case where the cutting runs between line 1 and 2. Obviously, the contribution 1(234) from above and below produces a diffractive cut, the remaining three contributions lead to a cut reggeon. Similarly the case where the cutting is between lines 3 and 4. Including sign and statistics we get the weight $-2/3!$ for the diffractive cut (for the explanation of the negative sign see the argument before eq.(18)), and $-2\cdot 3/3!$ for the contributions with a cut reggeon. From the term with cutting line between 2 and 3 we obtain only cut reggeon graphs, with weight $4/(2!)^2$. In the sum, all contributions with cut reggeons cancel, and we are left with the diffractive cut only: this is what we expect when we interpret these terms as three particle contribution to the (odd signature) gluon trajectory function.

We are finally left with another type of contributions, the “nondiagonal“ terms (Fig.16b). Here the reggeons from above and below do not match, and these terms represent cut reggeon-reggeon interaction vertices for which the AGK arguments of the previous section do not apply. Some of these contributions are nothing but cuts (in external masses) of the BFKL kernel: they are to be interpreted as another kind of “bootstrap“ mechanism in QCD. Other contributions represent new and higher order corrections to the BFKL kernel: in principle, it should be possible to derive in this way the corrections which have been studied in [17]. We hope to return this question in a future paper, and we will not discuss it in any more detail here.

In summary, we have seen that all contributions obtained from the set of QCD diagrams illustrated in Fig.14a fit into the AGK cutting rules; the only exception are the t-channel cuts of the four-reggeon vertices for which the AGK rules do not make any prediction. Compared to earlier studies, the new features in QCD are the reggeization of the gluon and, more general, the color degree of freedom.

6 Conclusion

In this paper we have reviewed the “old” space-time picture of multireggeon amplitudes and the physical interpretation of the AGK cutting rules, almost forgotten during the last 10-15 years. Our main interest was in the question of how these ideas are realized in perturbative QCD. As to the space-time picture of the scattering amplitude, our main new result is the appearance of a “change of the arrow direction”: an interaction between a pair of reggeons is accompanied by a change of the direction of time (Fig.8b,d). One of the reasons why, to our knowledge, this observation has not been made before is that the t-channel iteration of two-ladder states has not been studied very much; in QCD it was the calculation of the anomalous dimension of the four-gluon operator which motivated a careful study of these diagrams.

Our study of the AGK cutting rules in QCD has, once more, emphasized the importance of the reggeization of the gluon (bootstrap). In short, the QCD diagrams which contribute to the present level of approximation contain pieces which have to be counted as higher order corrections to the BFKL ladder diagrams. They have to be removed before we are ready to define four gluon states and the two-Pomeron exchange. As a result of this procedure, the (new) $2 \rightarrow 4$ gluon vertex emerges which has strikingly simple symmetry properties. Also, there is no direct coupling of the four gluon state to the quark pair, we are dealing with enhanced diagrams only. After this decomposition into reggeizing and irreducible parts it is straightforward to verify the AGK cutting rules for the two-ladder exchanges.

Moving into more detail of the AGK cutting rules, we have obtained a simple matrix which describes, inside the Pomeron-Pomeron interaction, the transition from one s-cut to another and which goes beyond the original AGK rule in (13). Namely, in order to satisfy the AGK rules the t-channel partial wave above and below the four gluon state have to be the same, no matter whether the s-cut runs between the lines 1 and 2, 2 and 3, or 3 and 4. Once this partial wave by itself contains two-reggeon states, it is a nontrivial question to ask how the weight of the different cuts is preserved inside the partial wave. Our answer to this question is contained in the matrix (19), and the AGK weights appear as an eigenvector to this matrix. This is a new result which has not been discussed before.

In summary, we feel that the space-time analysis of these rather complicated diagrams provides, despite all its subtleties, a fairly easy picture of elastic scattering and diffractive dissociation at high energies. It is also gratifying to see that the AGK rules are satisfied, even if in QCD some details are quite unexpected. As a next step, we believe, one should attempt to generalize the simple probabilistic interpretation of the one-ladder approximation. For diagrams with more than two t-channel lines one has, in addition to the familiar squares of one-parton wave functions, also non-diagonal elements of a density matrix. The precise formulation of such a density matrix requires many of the details presented in this paper.

Acknowledgement: One of us (M.R.) would like to thank DESY for its kind hospitality and the Volkswagen-Stiftung for financial support.

References

- [1] V.N.Gribov, B.L.Ioffe, I.Ya.Pomeranchuk, *Sov.J.Nucl.Phys.* **2** (1966) 549.
- [2] V.A.Abramovski, V.N.Gribov, O.V.Kancheli, *Sov.J.Nucl.Phys.* **18** (1974) 308.
- [3] D.Amati, S.Fubini, A.Stangellini, *Nuovo Cim.* **26** (1962) 826.
- [4] S.Mandelstam, *Nuovo Cim.* **30** (1963) 1113, 1127.
- [5] E.A.Kuraev, L.N.Lipatov, V.S.Fadin, *Sov. Phys. JETP* **45** (1977) 199;
Ia.Ia.Balitskii, L.N.Lipatov, *Sov. J. Nucl. Phys.* **28** (1978) 822.
- [6] V.N.Gribov, *Sov.Phys.JETP* **57** (1970) 709.
- [7] B.L.Ioffe, *Phys.Lett.* **B 30** (1969) 123.
- [8] L.V.Gribov, E.M.Levin, M.G.Ryskin, *Phys.Rep.* **100** (1983) 64.
- [9] A.P.Bukhvostov, E.A.Kuraev, L.N.Lipatov, *Sov.Phys. JETP* **60** (1984) 22.
- [10] G.V.Frolov, V.N.Gribov, L.N.Lipatov, *Sov.J.Nucl.Phys.* **12** (1970) 543.
- [11] J.Bartels, *Z.Phys.* **C 60** (1993) 471.
- [12] G.M.Cicuta, B.Hasslacher, D.K.Sinclair, R.L.Sugar, *Phys.Rev.Lett.* **25** (1970) 1591;
G.M.Cicuta, R.L.Sugar, *Phys.Rev.* **D 3** (1971) 970; B.Hasslacher, D.K.Sinclair, *Phys.Rev.*
D 3 (1971) 1770.
- [13] J.Bartels, M.Wüsthoff, *Z.Phys.* **C 66** (1995) 157.
- [14] V.N.Gribov: *Sov.Phys.JETP* **26** (1968) 414.
- [15] J.Bartels, L.N.Lipatov, M.Wüsthoff, *Nucl.Phys.* **B 464** (1996) 298.
- [16] E.M.Levin, M.G.Ryskin, *Sov.J.Nucl.Phys.* **20** (1975) 280.
- [17] C.Coriano, A.R.White, *Phys.Rev.Lett.* **74** (1995) 4980; *Nucl.Phys.* **B 451** (1995) 231;
Nucl.Phys. **B 468** (1996) 175; *Nucl.Phys.* **B 451** (1996) 219.

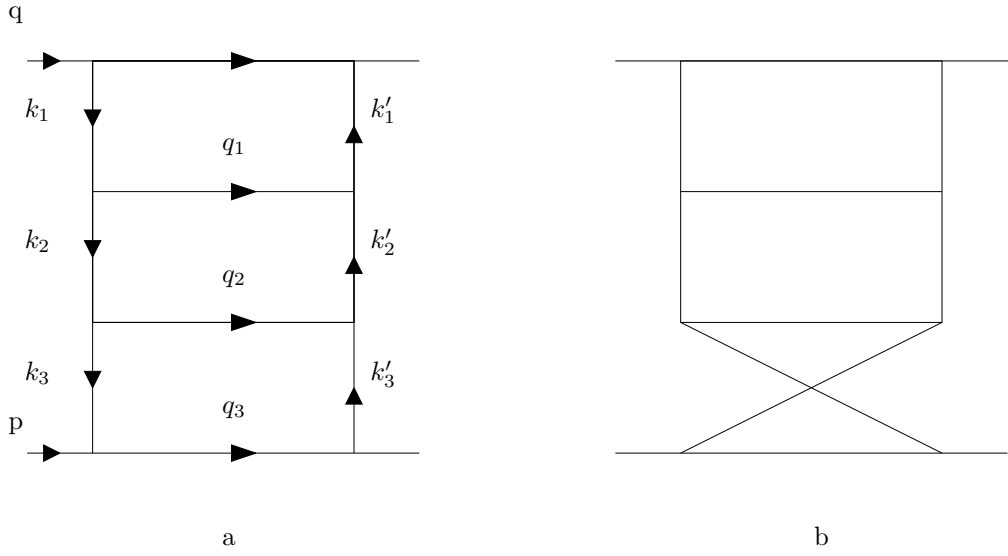


Figure 1: (a) Single Ladder exchange; (b) Crossed ladder

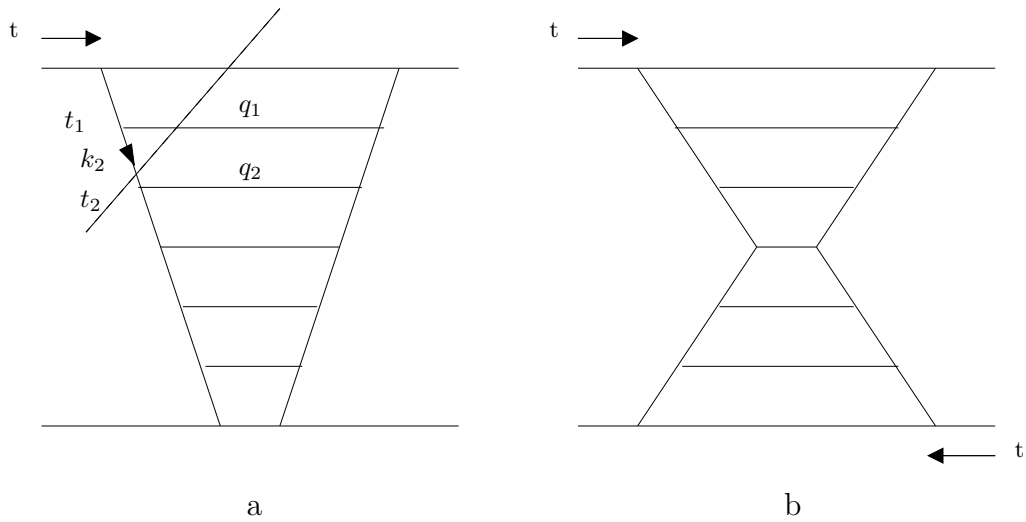


Figure 2: (a) Time ordering in the proton rest frame. The cutting line illustrates an intermediate state in non-covariant perturbation theory; (b) time ordering in the cm-system

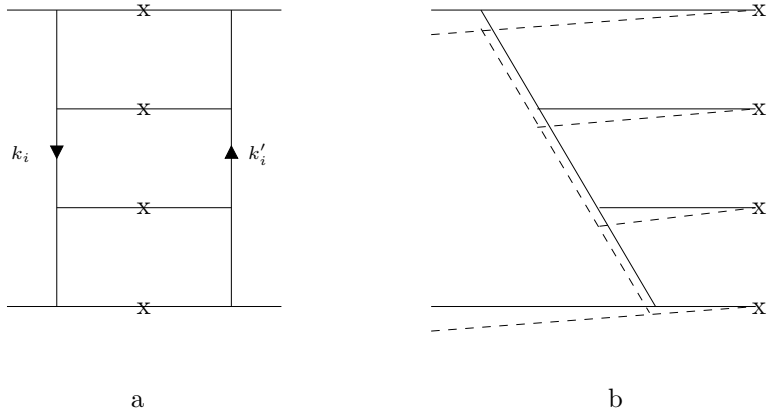


Figure 3: Time ordering of the imaginary part of a single ladder: (a) the energy discontinuity of Fig.1a; (b) the time ordering of the energy discontinuity

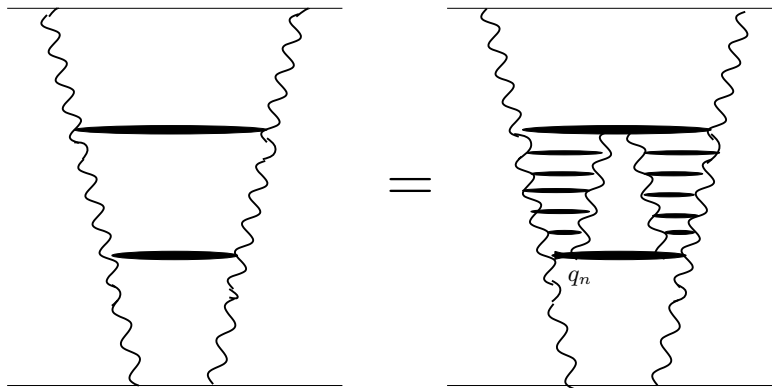


Figure 4: A reggeon diagram in QCD. The wavy lines denote reggeized gluons, the black rung stands for the BFKL kernel. The right hand part illustrates the space time structure of a reggeized gluon which, because of the bootstrap property, can be redrawn as a ladder-like insertion

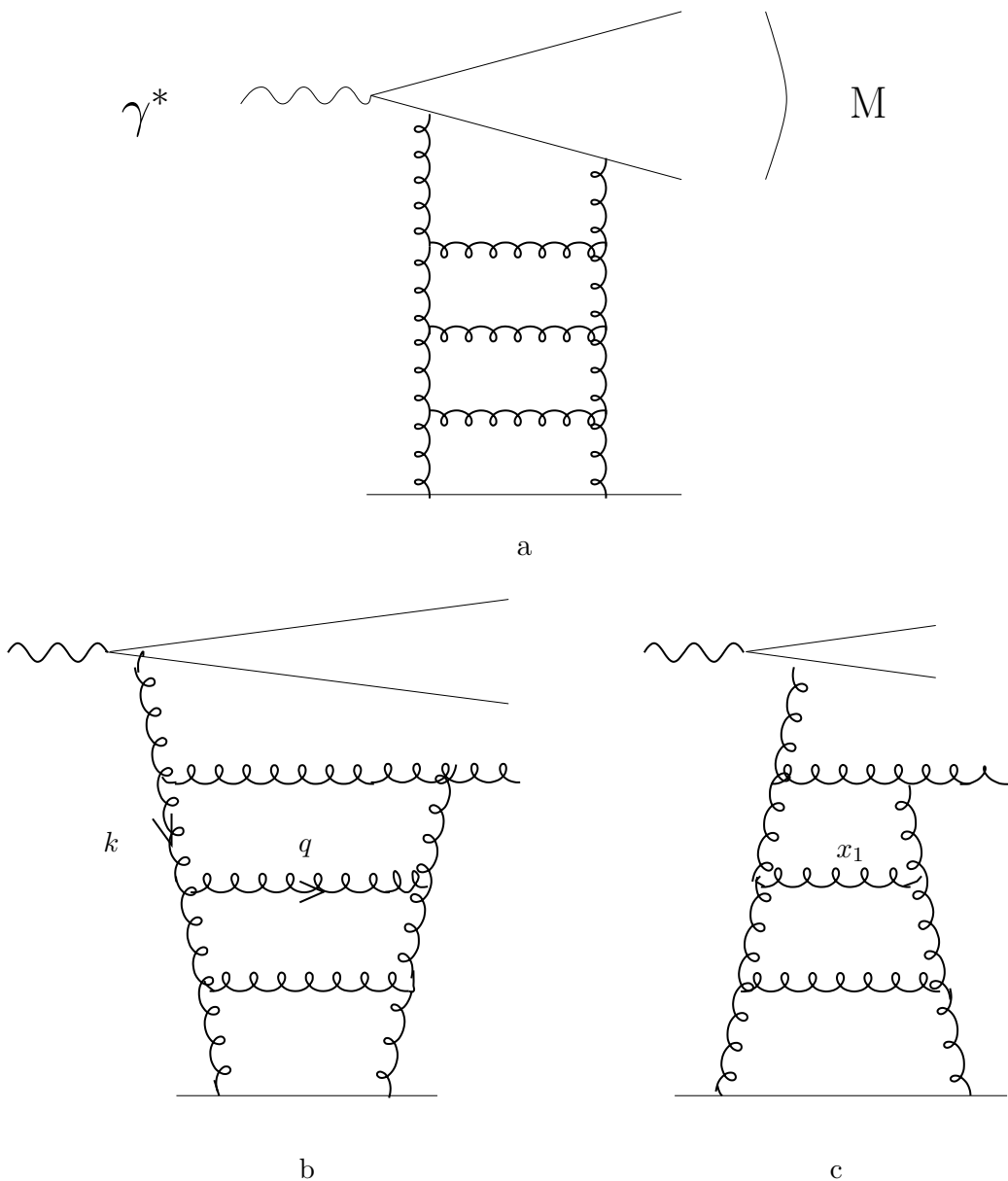
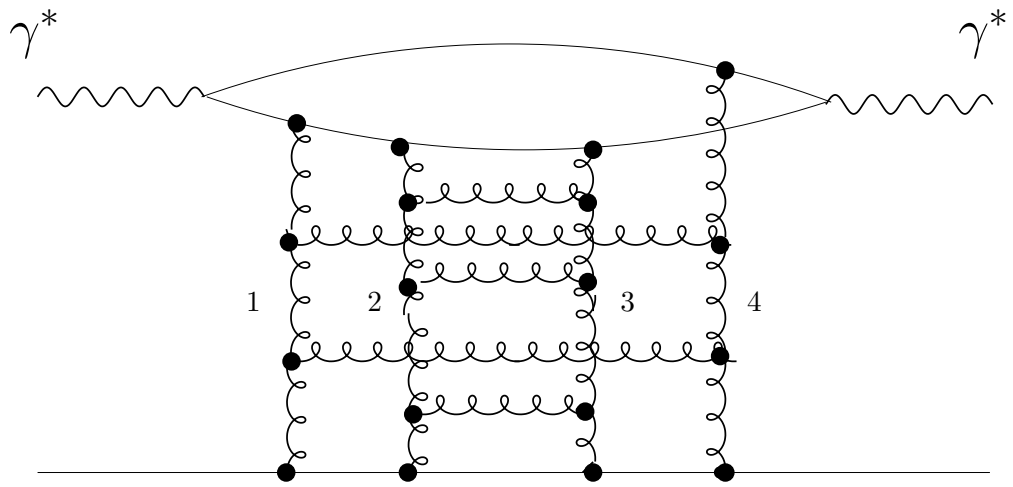
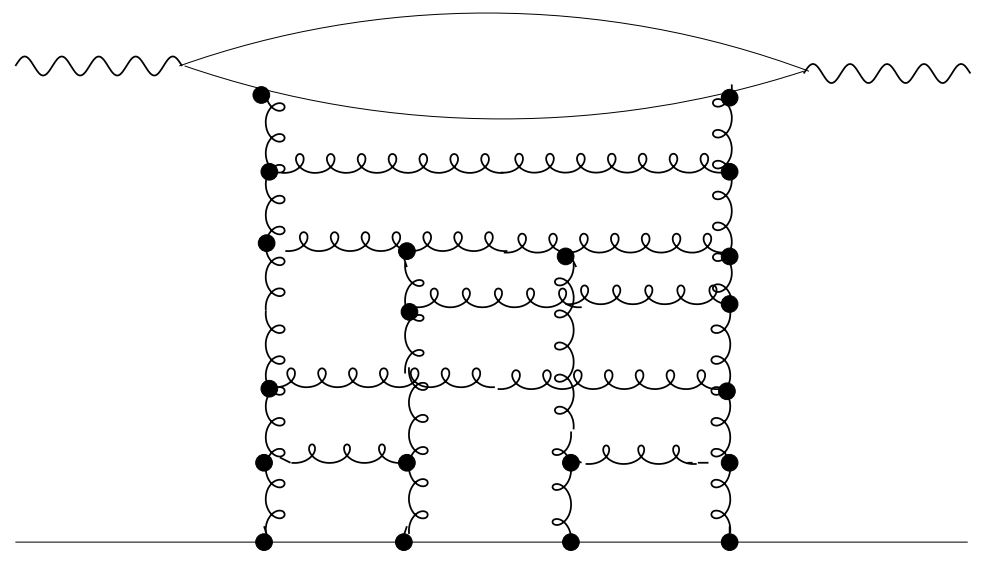


Figure 5: (a) Single ladder exchange in diffractive dissociation (wavy lines denote gluons); (b) time ordering in the target rest frame; (c) time ordering in the Breit frame

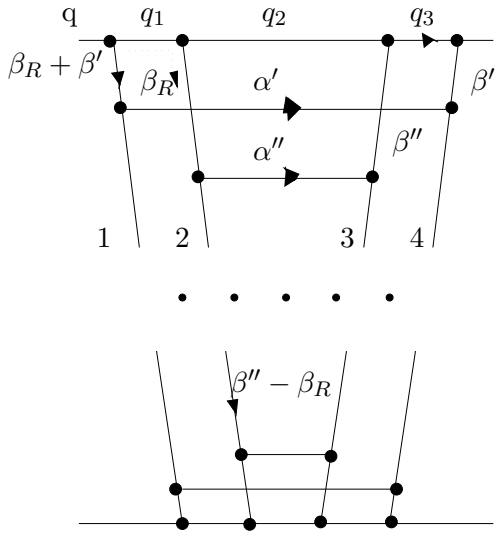


a

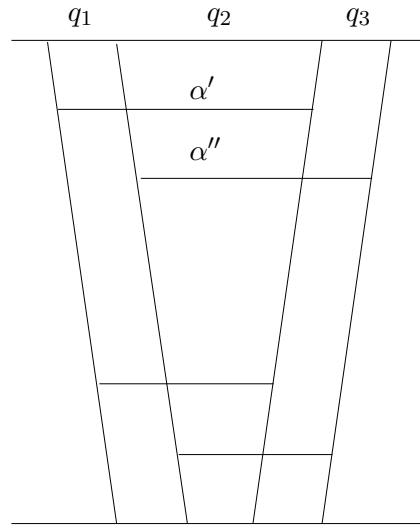


b

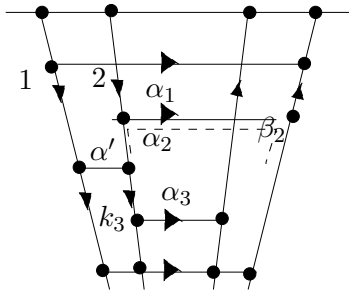
Figure 6: Double ladder exchange (wavy lines denote gluons): (a) the simplest two-ladder diagram; (b) a more general example (enhanced diagram)



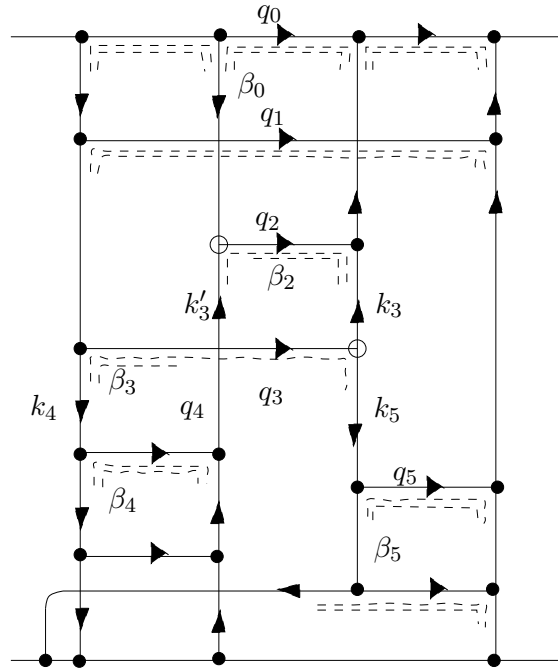
a



b



c



d

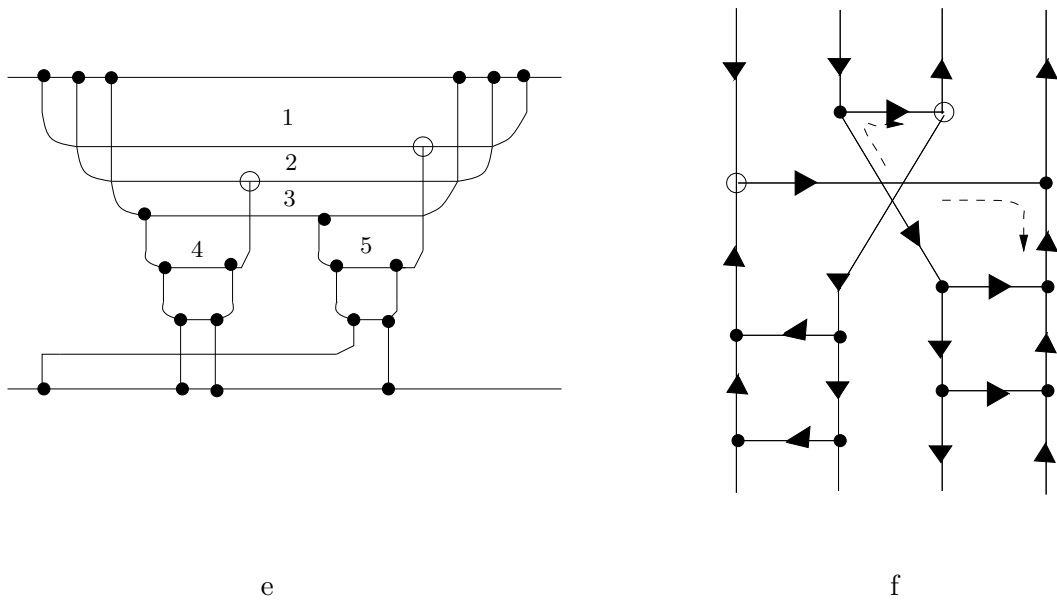


Figure 7: Diagrams with four t-channel lines. (a) maximal nested structure at the upper end; (b) example of a non-nested structure which does not contribute to the leading log approximation; (c) example of a switch which vanishes at high energies; (d) example of a switch for which a change of the time direction on line 2 and 3 gives a nonvanishing contribution. Vertices at which time changes its direction are marked by circles; (e) the space time structure of (d); (f) an example of a crossed diagram which contributes at high energies

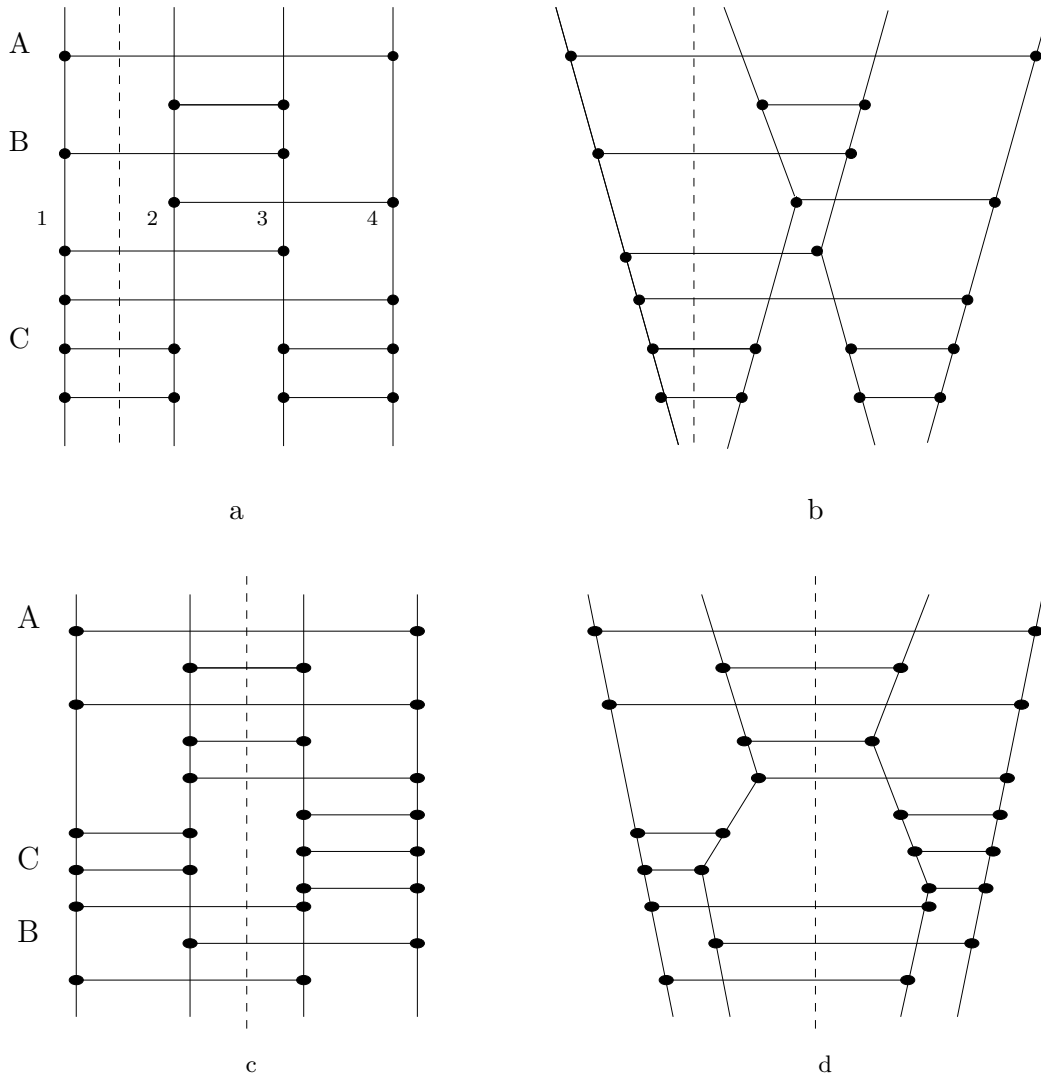


Figure 8: Two more examples of nonvanishing contributions ((a) and (c)) with their space-time structure ((b) and (d), resp).

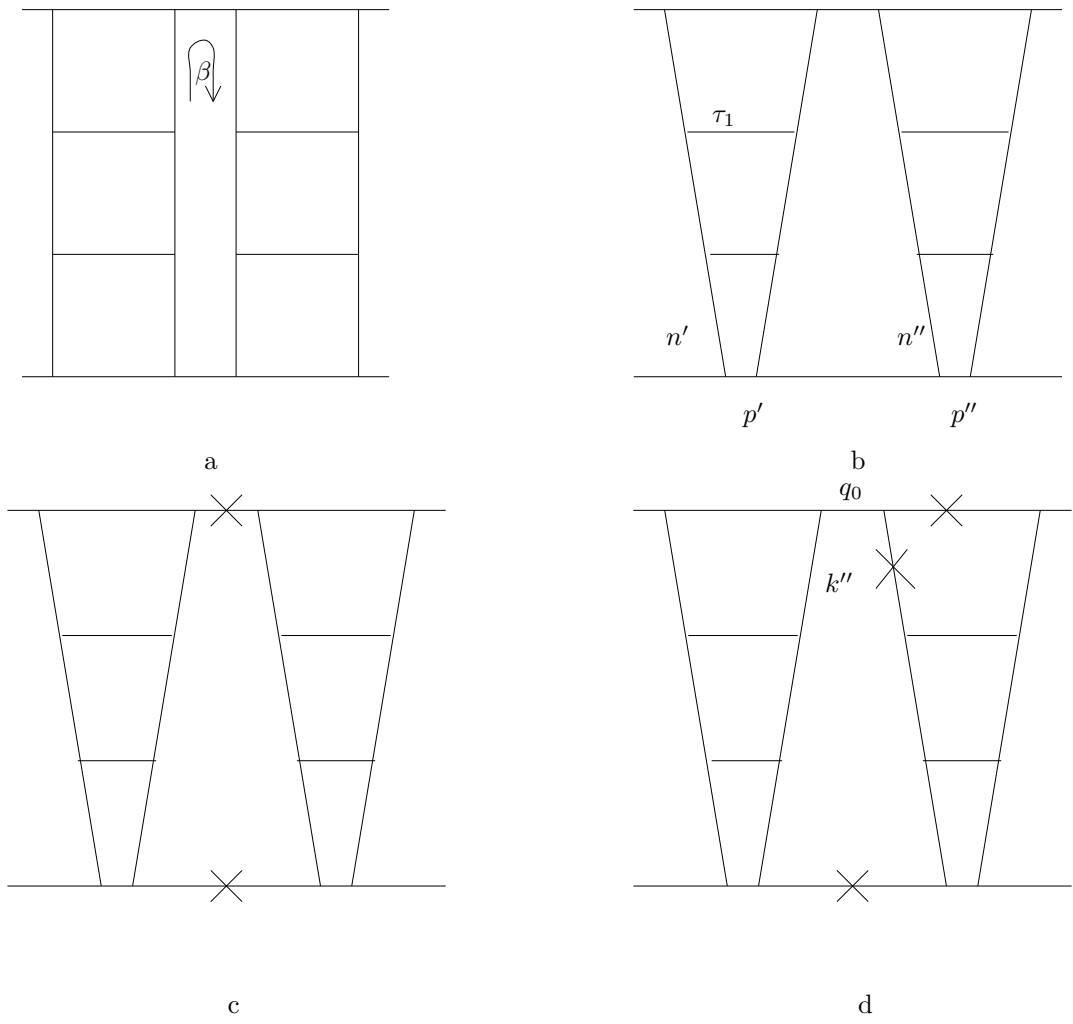


Figure 9: The AFS diagram (planar coupling of two ladders to the upper line): (a) the Feynman diagrams; (b) space time structure of (a); (c) the elastic intermediate state; (d) another intermediate state, which together with its hermitian conjugate, cancels against Fig.9c

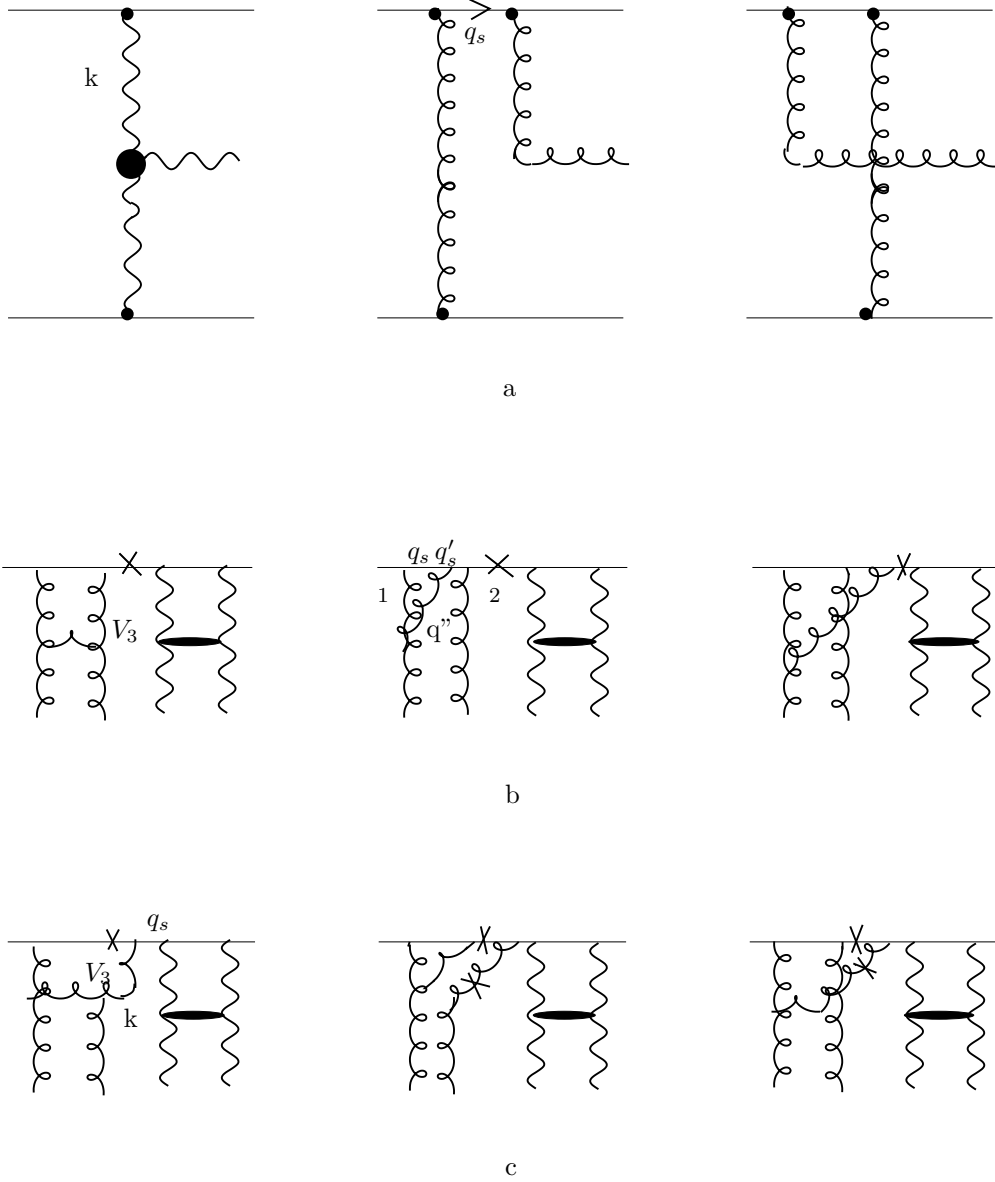


Figure 10: (a) Feynman diagrams which go into the BFKL production vertex; (b) the single particle cut in the AFS diagram in QCD: wavy lines denote gluons, the black rung the BFKL vertex. Inside the left hand side ladder, the BFKL rung has been resolved according to Fig.10a; (c) one of the two-particle cuts which cancels against the single-particle cut in (b)

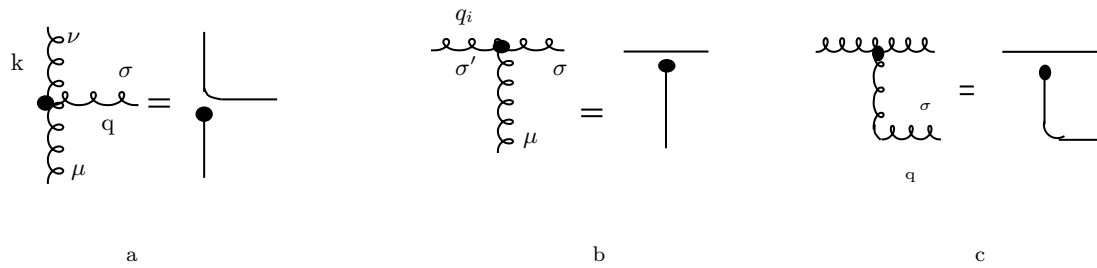


Figure 11: Momentum structure of the triple gluon vertex

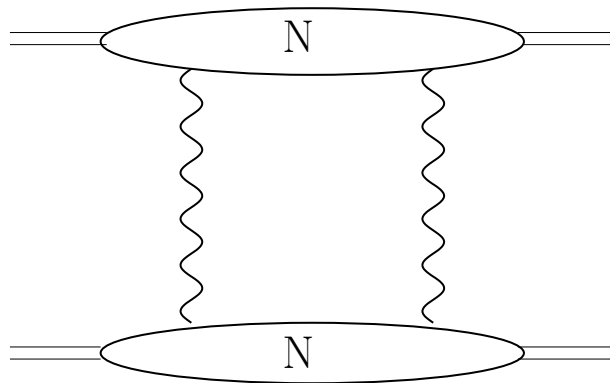


Figure 12: A general two-reggeon exchange amplitude (wavy lines denote reggeons)

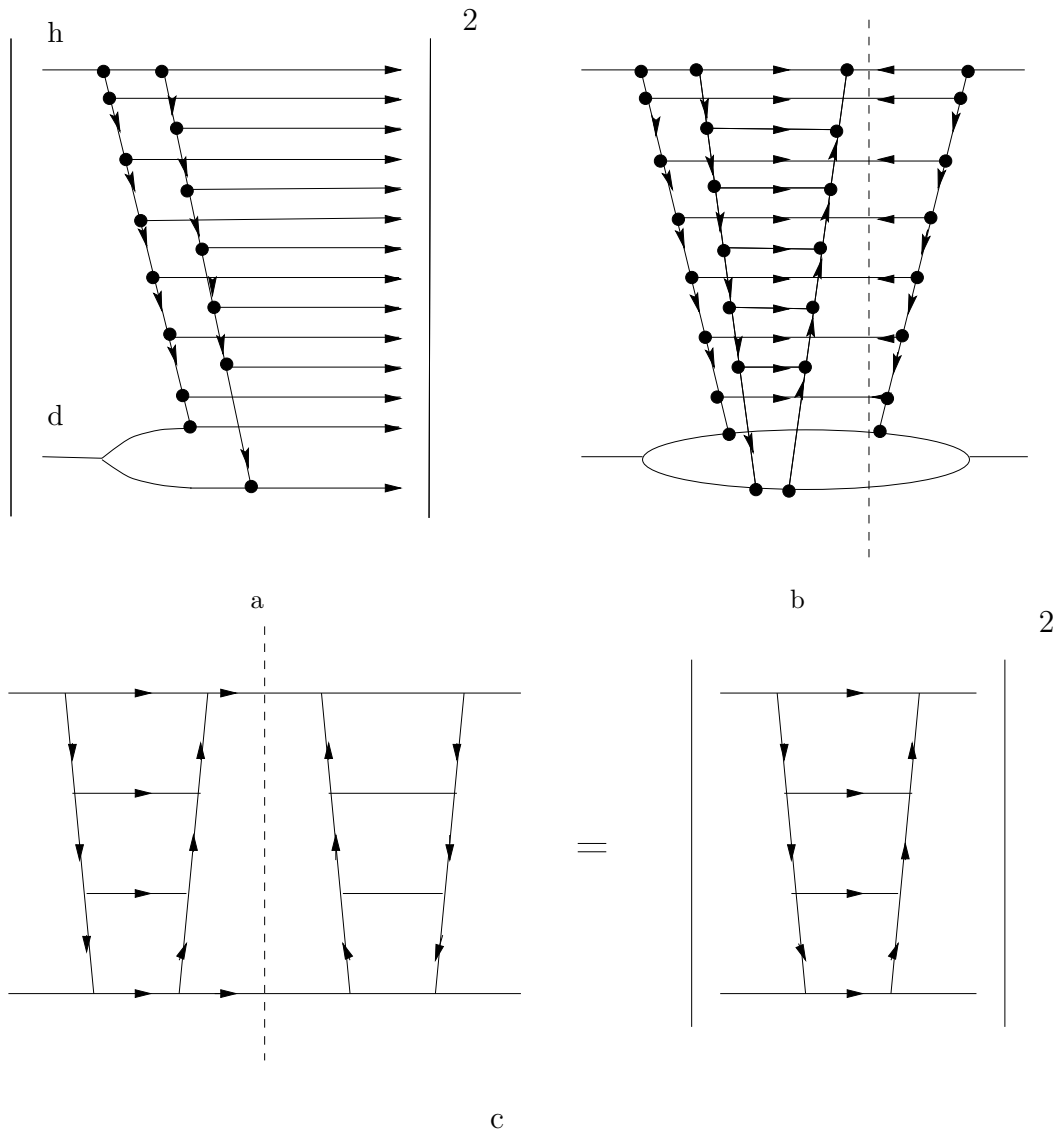
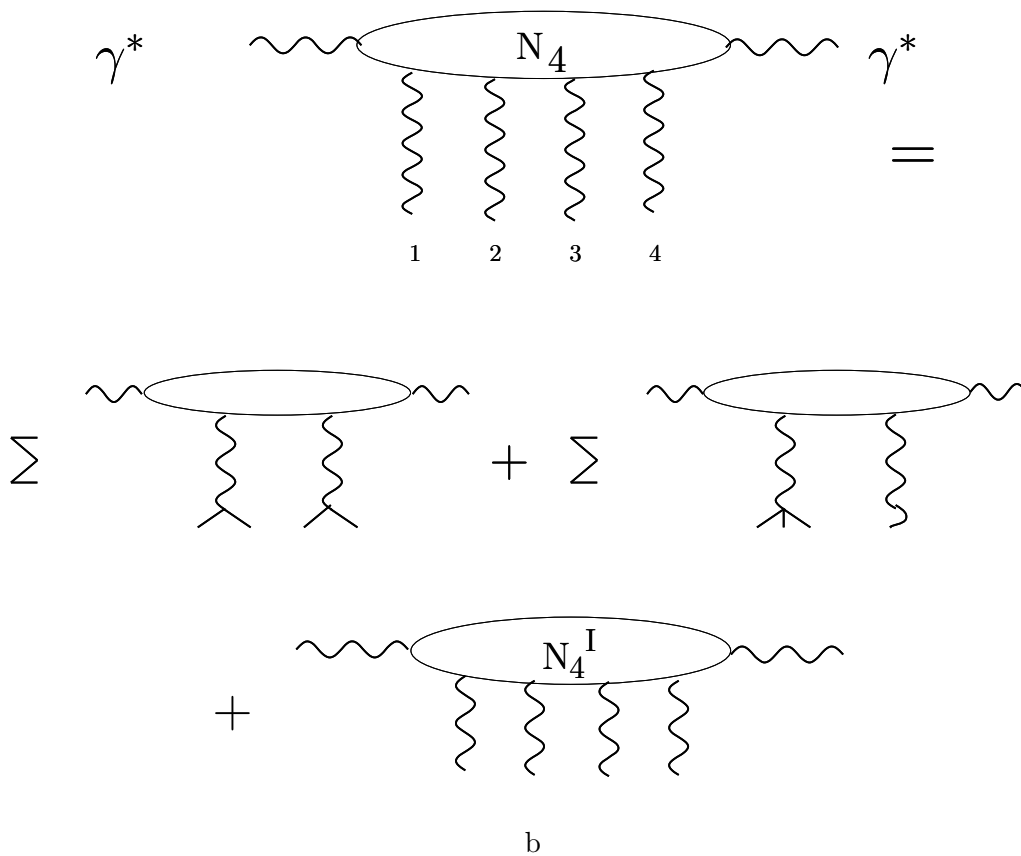
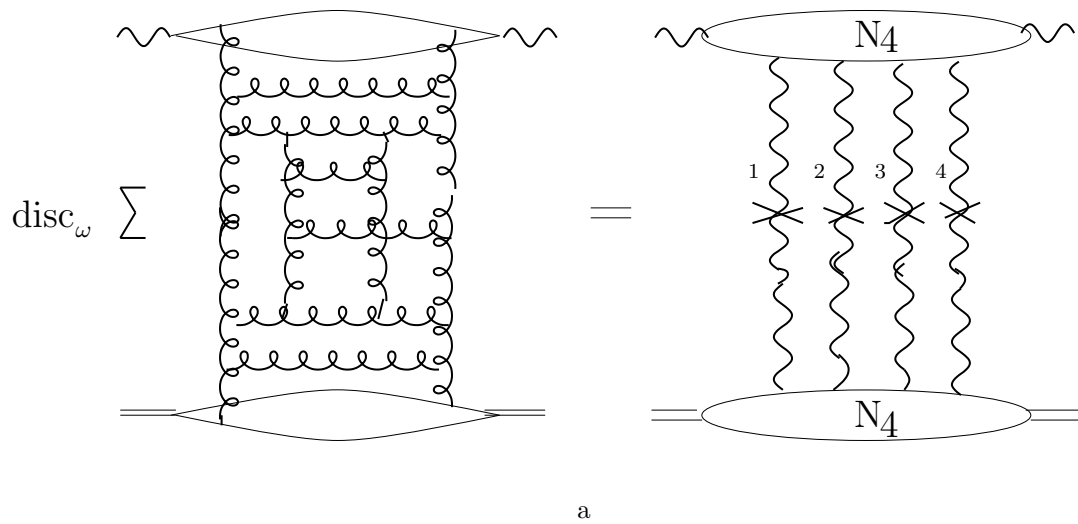


Figure 13: Space time structure of the corrections to the scattering of a hadron on a deuteron target: (a) final states with double multiplicity; (b) single multiplicity final state; (c) the diffractive cut



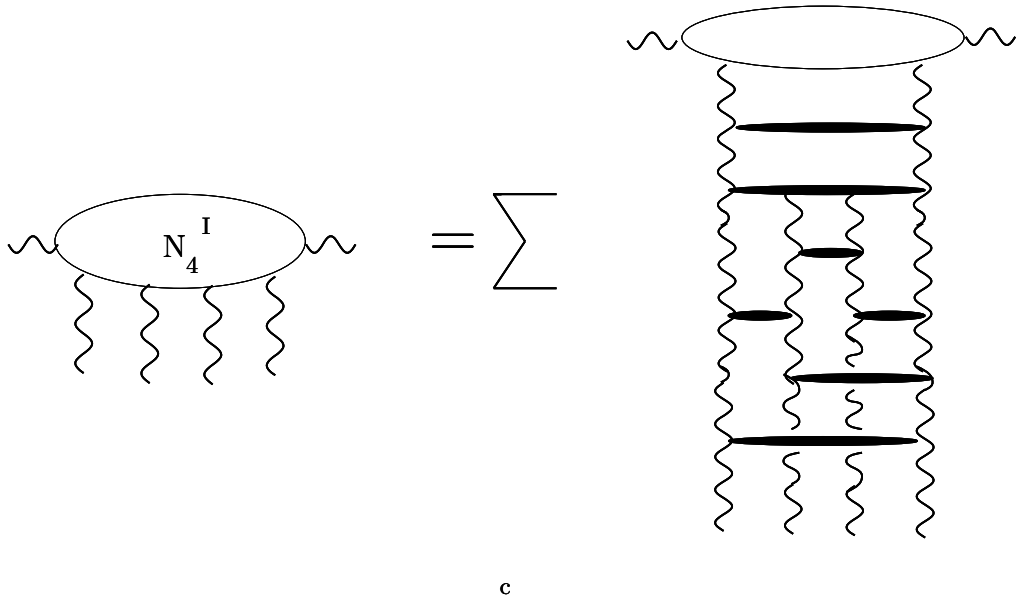


Figure 14: (a) General QCD gluon diagram with a four gluon state; after summing, on the left hand side, over all contributions the sum of all diagrams can be drawn in terms of effective (BFKL) vertices and reggeized gluons. The discontinuity refers to angular momentum in the t-channel. (b) decomposition of the partial wave N_4 with four reggeized gluons into the reggeizing part and the irreducible part; (c) illustration of the irreducible part

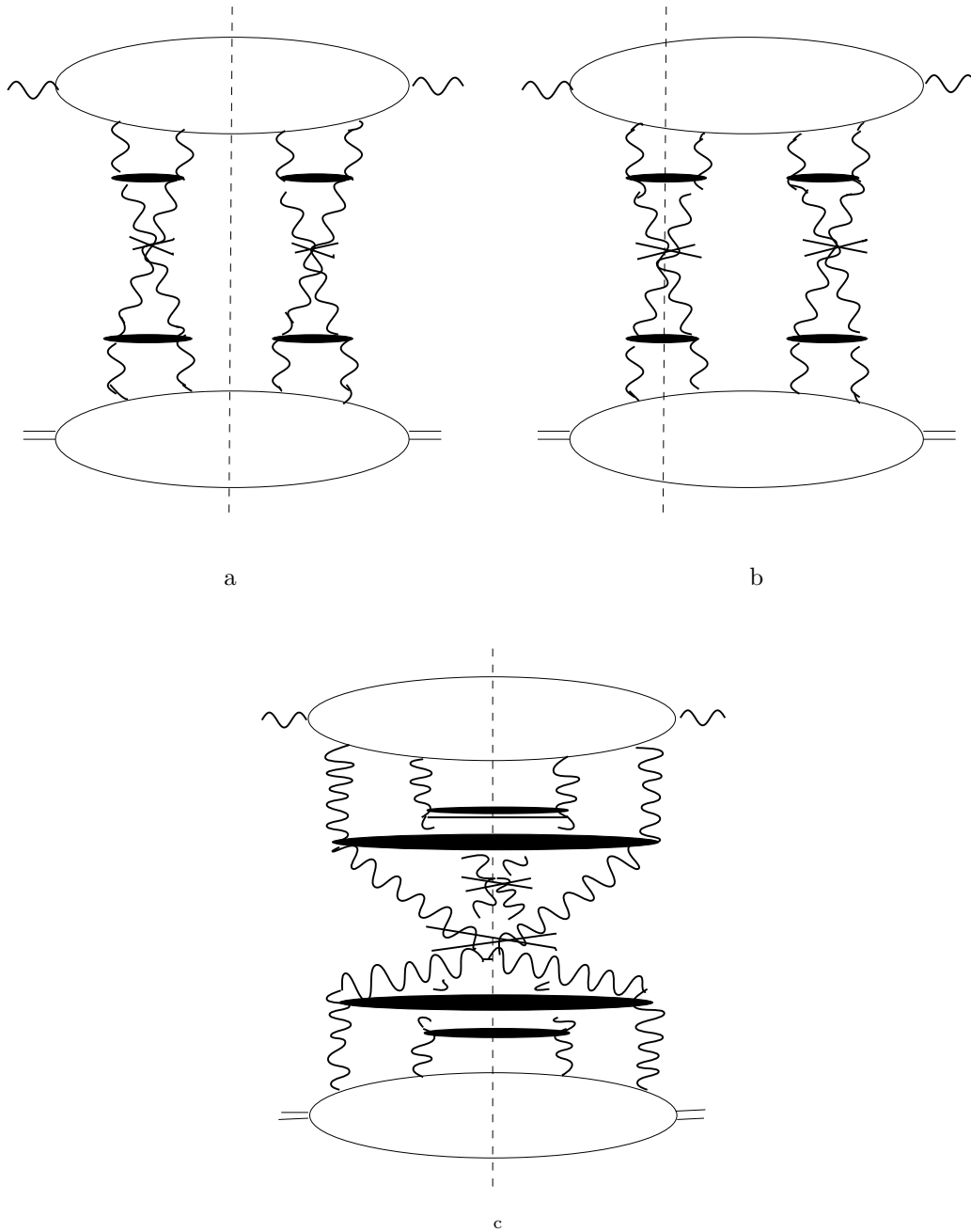


Figure 15: The AGK counting rules for the ladder states: (a) the diffractive cut σ_0 ; (b) the multiperipheral cut σ_1 ; (c) the double multiperipheral cut σ_2

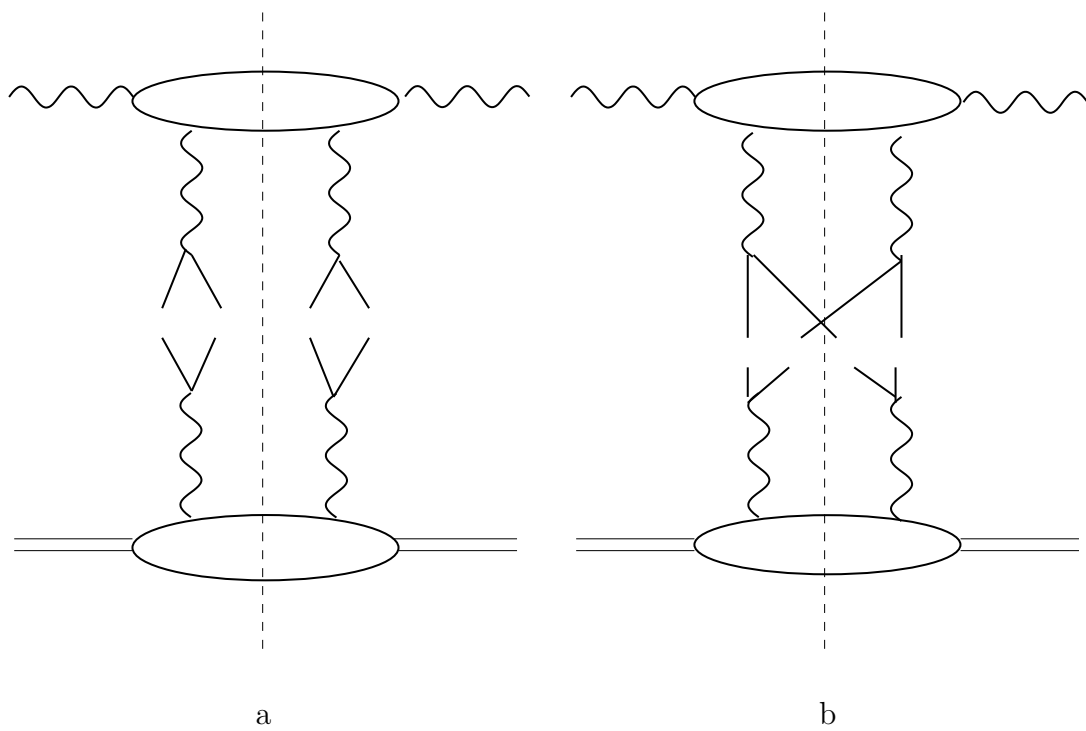


Figure 16: Contribution of the reggizing pieces to the t-channel discontinuity. (a) a “diagonal term“ which matches eq.(8); (b) a “nondiagonal term“ which is interpreted as a t-discontinuity of a four reggeon vertex